River alkalinity enhancement for scalable and energy-efficient geochemical carbon dioxide removal: potential, costs and risks?

Authors:
Arthur Vienne, Tom Cox, Harun Niron, Michele Moretti, Tim Jesper Suhrhoff, Sara Vicca

Abstract

Gigaton-scale carbon dioxide removal (CDR) from the atmosphere will be necessary to limit global warming to below 2 °C. Current approaches, such as afforestation or biochar, are constrained by land and biomass availability, whereas direct-air carbon capture technologies are energy-intensive and costly. Here, we discuss river alkalinity enhancement (RAE), a geochemical carbon dioxide removal strategy that uses readily available limestone ($CaCO_3$) and derived slaked lime ($Ca(OH)_2$) to increase alkalinity in rivers. Unlike the direct addition of these minerals to the ocean, which is currently restricted by the London protocol, addition of alkalinity to rivers is already commercially applied in some regions and alkalinity dosing can be monitored in controlled systems. Controlled rock dissolution in ponds allows for direct measurement of CO_2 removal prior to water release back into rivers, enhancing traceability and verification.

We simulate CO_2 uptake in 149 major rivers, considering river flows and chemistry and life-cycle emissions from mining, grinding and transporting rock and pumping water in reactor ponds. Our results indicate that RAE using $CaCO_3$ in these rivers could remove an upper limit of over 0.2 but below 0.4 gigatons of CO_2 per year, yet over 1 gigaton CO_2 per year using $Ca(OH)_2$, even after subtraction of major process emissions. Estimated costs may be below $200 per ton of carbon dioxide removed, substantially lower than conventional energy-intensive direct-air capture approaches. Nonetheless, the ecological risks and potential alteration of photosynthesis by aquatic plants after RAE-induced pH and alkalinity increases should be thoroughly investigated prior to widescale RAE adoption. If ecological risks would be minor, RAE may offer a scalable, relatively energy-efficient and economically viable pathway for geochemical CDR, while also delivering the co-benefit of mitigating ocean acidification downstream.

1. Introduction

Gigatons of carbon dioxide removal (CDR) will be needed in order to keep global warming below 2°C (IPCC, 2023). Besides biomass-based CDR (e.g. afforestation and biochar), proposed CDR techniques include energy-intensive direct-air carbon capture and storage (DACCS), direct ocean capture and geochemical CDR. Geochemical CDR refers to a broad range of approaches that aim to sequester CO_2 as solid and/or dissolved inorganic C, using minerals.

Several existing geochemical CDR approaches include Mineral Carbonation (MC), terrestrial/coastal Enhanced Weathering (EW) and ocean liming each with their distinct limitations. Alkalinity reflects the capacity of water to neutralize acids through base ions such as bicarbonate and carbonate that buffer pH. Higher alkalinity allows greater CO_2 uptake because these ions shift the carbonate equilibrium toward stable carbonate forms, rather than free carbonic acid.

CDR using MC involves the formation of solid carbonate rocks, which is a relatively energy-intensive geochemical CDR approach (Keith et al., 2018; Kelemen et al., 2020). Terrestrial EW consumes less energy and aims to transport dissolved inorganic C (DIC) from soils through groundwater, river catchments, to the ocean eventually. This DIC transport may however be less effective than initially anticipated. First, rock dissolution may be slower than previously thought (Power et al., 2025). Secondly, once rocks are dissolved, there may be a significant lag time (in the order of decades) before atmospheric CO_2 is effectively removed and DIC eventually increases in the ocean (Kanzaki et al., 2025).

Mechanistically, complex processes in soils (base cation exchange, cation adsorption associated with soil organic C (SOC), Fe (hydr)oxides and clay formation) could all retard the efflux of base cations and DIC to the ocean (Kanzaki et al., 2025; Steinwidder et al., 2025; Vienne et al., 2024).

A critical challenge for terrestrial EW is the CDR quantification, leading to high costs for monitoring reporting and verification (MRV). In EW, MRV can account for over 50% of the cost for CDR (Mercer et al., 2024). Furthermore EW can significantly influence organic C in soils by altering microbial activity (e.g. through pH neutralization (Klemme et al., 2022; Dietzen et al., 2018)), which is a critical consideration given that SOC stocks and their associated fluxes typically exceed inorganic carbon dynamics by an order of magnitude in agricultural soils (Clarkson et al., 2024). Although terrestrial EW may come with multiple benefits for crop growth (Beerling et al., 2018), it is also associated with a risk for heavy metal pollution. The (ultra)mafic rocks that are proposed for EW can e.g. contain Ni, Cr and Cu, which may pose a risk to human health if they enter the food chain (Dupla et al., 2023).

Applying rocks in the oceans through ocean liming and coastal EW rather than on land can reduce reliance on widespread land-based distribution, thereby mitigating one of the key logistical challenges of terrestrial EW: extensive land transport (Fan et al., 2018; Lefebvre et al., 2019). In coastal EW – which aims to apply rocks, mostly ultramafic sands, to sediments using ships – some of the challenges of terrestrial EW are mirrored. Coastal EW relies on the same, relatively slow dissolution kinetics of ultramafic minerals, monitoring marine CDR is highly model-dependent due to the complexity of ocean systems and heavy metal leaching may pose a risk for ecosystems and food webs (Flipkens et al., 2021). Last, there is a significant legal barrior: 'the London protocol', which essentially prohibits addition of chemicals to the ocean, inhibiting the adoption of marine geochemical CDR in practice (Warbrick et al., 1997). Disadvantages related to dissolution kinetics and heavy metals in ultramafic rocks have driven the marine geochemical CDR community to explore alternative feedstocks: carbonate derivatives ($Ca(OH)_2$, $Mg(OH)_2$, or hydrous carbonates such as ikaite), with distinct advantages and drawbacks (Kowalczyk et al., 2024; Renforth et al., 2022). Not only are the carbonate(-derivatives) safer than ultramafics in terms of heavy metal contamination, their dissolution rates are multiple orders of magnitude higher (Palandri & Kharaka, 2004). Moreover, while global dunite reserves are estimated at several tens of Gtons (Geerts et al., 2025), current annual mining yields only 8.4 Mtons of olivine, which is three orders of magnitude less than the 6.6 Gtons of $CaCO_3$ mined annually (Caserini et al., 2022).

Ocean liming approaches with carbonate-derivatives however also have major disadvantages: they consume substantial amounts of energy, producing hydroxides requires carbon capture and storage (CCS) and CO_2 removal could be reversed if too much rock is added at once and carbonates precipitate. Naturally carbonate-derivatives are scarce: current brucite ($Mg(OH)_2$) extraction is only 1.5 Mt $year^{-1}$ (Caserini et al., 2022). To scale beyond megatons of CDR, carbonate-derivatives need to be produced artificially from carbonates, consuming substantial energy inputs (Kowalczyk et al., 2024). In addition, producing 1 mol hydroxides from a mol of carbonate (calcination process) inherently emits 1 mol of CO_2 ($CaCO_3 \rightarrow CaO + CO_2$ and $CaO + H_2O \rightarrow Ca(OH)_2$). During the dissolution of 1 mol $Ca(OH)_2$, 2 mols of CO_2 are theoretically sequestered again, resulting in a theoretical maximum of 1 mol CO_2 sequestered per mol carbonate without CCS. Yet, if CCS is used, the CO_2 produced during calcination can be captured and 1 mol carbonate can theoretically capture 2 mol.

Achieving climate targets will require gigaton-scale CDR, yet many proposed approaches face significant technical, environmental, legal and economic constraints. In addition to the terrestrial and marine environment, a third environment where geochemical CDR can be implemented is in rivers, through 'river alkalinity enhancement (RAE)'.

RAE could have substantial advantages over terrestrial/marine geochemical CDR due to advantages associated with logistics, energy use, simplified MRV and legal frameworks. We envisage a system where coastal carbonate rocks are transported to rivers through water-way transport. First, C-intensive land transport is minimized in this geochemical CDR strategy. Secondly, carbonates can dissolve in many rivers (Knapp & Tipper, 2022) without an external CO_2 supply, while oceans are oversaturated in $CaCO_3$ (Batchelor-McAuley et al., 2022) and would require additional CO_2 (e.g. from organic sediments

or industry) to dissolve carbonates. When no external concentrated CO_2 source is present, carbonates can only dissolve in the ocean after energy-intensive conversion into carbonate-derivatives. Hence, if carbonates rather than carbonate-derivatives can be used for RAE, this could reflect in substantial energy savings. Thirdly, in rivers, controlled systems such as reactor ponds or existing infrastructure such as wastewater treatment plants (WWTPs) could be used to control alkalinity release, offering significant advantages for MRV. In such closed system, sensor-based MRV could enable real-time tracking of dissolved cations and CO_2 uptake, improving transparency and trust in carbon accounting. For instance, electrical conductivity sensors can serve as low-cost proxies for DIC (Amann & Hartmann, 2022). Last, to the best of our knowledge, no legislative barriers such as the London protocol exist for rivers.

Despite all these theoretical advantages, RAE has received limited attention in scientific literature, with only few studies addressing its potential (Cai & Jiao, 2022; Köhler et al., 2010; Rønning, 2024). Previous studies have explored different implementation strategies. Rønning (2024) suggested adding olivine to rivers, whereas Cai & Jiao (2022) and Köhler et al. (2010) suggested liming of wastewater and rivers. Sterling et al. (2023) presented a perspective on the direct addition of limestone to rivers using automated limestone dosing tanks, hereafter referred to as 'direct-river liming'. To improve the monitoring of rock dissolution, an alternative approach involves the use of near-river ponds, allowing for more controlled conditions. This method is hereafter termed 'pond-river RAE' (**Figure 1**). In addition to application methods, the chemistry of the applied mineral matters: while $CaCO_3$ can enhance alkalinity in undersaturated rivers but only dissolves up to saturation, $Ca(OH)_2$ can offer greater overall CDR potential because it can raise water alkalinity beyond saturation with $CaCO_3$.

Being an emerging CDR strategy, RAE faces several critical knowledge gaps that must be addressed to determine its long-term viability. Chief among these are its global scalability and net CDR sequestration potential, particularly once major life-cycle emissions are accounted for. Secondly, the resource intensity—specifically the land, water, and energy requirements—remains poorly quantified. Thirdly, the cost of CDR through RAE has – to the best of our knowledge - not been estimated yet through techno-economic assessment (TEA). Finally, the environmental and reversal risks and potential trade-offs of large-scale implementation are yet to be rigorously evaluated, necessitating a comprehensive assessment of the technology's safety and efficacy. Therefore, this study investigates the abovementioned aspects of RAE in four scenarios. Scenario 1: pond-river $CaCO_3$; scenario 2: pond-river $Ca(OH)_2$; scenario 3: direct-river $CaCO_3$ and scenario 4: direct-river $Ca(OH)_2$ (**Figure 1**).

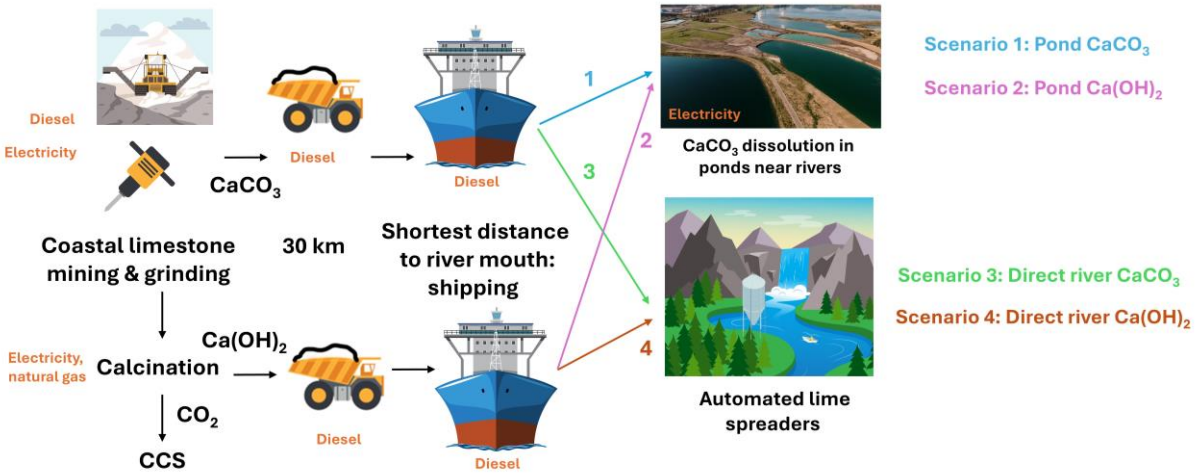

Figure 1: Overview of the Techno-economic assessments (TEA) used to quantify the cost per unit of net CDR. Four scenarios (pond river liming, pond river $Ca(OH)_2$ application, direct river liming, and direct-river $Ca(OH)_2$ application) are considered. A more detailed process scheme can be found in **Figure S9**. CCS = Carbon capture and storage.

2. Materials and Methods

2.1 PHREEQC simulation 1: quantifying the CDR potential and water needs to dissolve $CaCO_3$ in rivers of the GEMS-GLORI database.

In a first simulation, we evaluate the CDR potential and water use to dissolve $CaCO_3$ in the rivers. River water chemistry, temperature and discharge data were obtained from the GEMS-GLORI database (Meybeck & Ragu, 1997). The dataset includes 555 large rivers selected based on at least one of the following criteria: discharge >10 km³ yr⁻¹, sediment discharge >5 Mt yr⁻¹, or basin population >5 million. This dataset covers 149 of Earth's largest rivers, used in this analysis, representing 55% of global runoff with 21,000 km³ yr⁻¹ (Fekete et al., 2002; Knapp & Tipper, 2022).

Inputs from the GEMS-GLORI database were entered in PHREEQC (Parkhurst & Appelo, 2013), using the *phreeqc* package in R-studio (R v4.3.2) with the PHREEQC.DAT database. Major ion concentrations (Ca^{2+}, Mg^{2+}, Na^{+}, K^{+}, SO_4^{2-}, HCO_3^{-}, Cl^{-}) and mean annual temperature were extracted and used as input for the PHREEQC SOLUTION function. Following the GEMS-GLORI dataset by Knapp & Tipper (2022), we only used rivers from GEMS-GLORI with measured HCO_3^{-} data. To account for the Congo River, the worlds' second-largest river by discharge but absent from GEMS-GLORI, chemistry data were added from the HYBAM database (http://www.ore-hybam.org). In the PHREEQC EQUILIBRIUM_PHASES function, we entered riverine pCO_2 in log(atmospheres) and calcite mass for equilibrium calculations. Note that annual averages for pCO_2 are used, while in reality pCO_2 can fluctuate due to seasonality effects.

$CaCO_3$ can only dissolve and hence deliver CDR if it is undersaturated in a solution, which requires a substantial dilution factor. Ultimately, the potential of river liming for CDR is limited by the annual discharge of $CaCO_3$-undersaturated rivers. To quantify the water required to dissolve $CaCO_3$ under varying riverine pCO_2 and chemistry, we used PHREEQC and calculated the chemical equilibrium (Parkhurst & Appelo, 2013). Using an iterative approach, additional river water volume (V) was added to a fixed mass of $CaCO_3$ solution in 1000 L increments, continuing until >99.99% of $CaCO_3$ was dissolved.

We extracted the following outputs from the simulation: volume V (m³), the saturation index (SI) of calcite, pH, CO_2 and total alkalinity (TA) of river water before and after adding the $CaCO_3$. V represents the required volume to dissolve 1 t $CaCO_3$. ΔCO_2 is a mass of gaseous CO_2 decrease obtained afer $CaCO_3$ addition up to saturation. From the outputs ΔCO_2, dissolution volume V, and the annual river discharge Q, the gross CDR potential was determined for the rivers as in **Equation 1** for rivers undersaturated in calcite (oversaturated rivers had a CDR potential of 0 in this simulation).

$$\text{Gross CDR potential } [\text{t } CO_2] = \frac{\Delta CO_2 \text{ (t)}}{\text{V [m3]}} * \text{Q} \left[\frac{\text{m}^3}{\text{year}}\right] * \eta \qquad \textbf{Eq. 1}$$

Simulated CDR may however be reduced by downstream oceanic carbon losses. No losses occur if ocean alkalinization efficiency is 100% ($\eta = 1$). A more conservative assumption is that all alkalinity is exported to the ocean, where part degasses according to the carbonate equilibrium ($\eta \approx 0.7$ mol CO_2 mol^{-1} TA, assumed for oceans) (Renforth et al., 2012; Renforth et al., 2019; Renforth & Henderson, 2017). Reported values of η range from 0.7–0.85 (Renforth et al., 2019), while model studies suggest 0.65–0.8 mol CO_2 mol^{-1} TA (see section S6 in the supplement of (Kowalczyk et al., 2024)). Therefore, we corrected for ocean alkalinity losses using endmembers of this range (η=0.65 and η=0.85) and adjust simulated CDR according to **Equation 1**.

2.2 PHREEQC simulation 2: quantifying the CDR potential of rivers in GEMS-GLORI for RAE with $Ca(OH)_2$

A second simulation quantifies the CDR potential and water requirements for $Ca(OH)_2$ addition across diverse river systems, using the critical saturation threshold (Ωc) as the upper operational limit (Zhang

et al., 2022). The saturation state (Ω) is the ratio of the ion activity product to the mineral's solubility product. While Ω > 1 denotes oversaturation, $CaCO_3$ precipitation typically only initiates once a higher critical threshold Ωc is reached (Moras et al., 2022). This threshold is a "break point" for precipitation: exceeding it triggers the precipitation of $CaCO_3$ and the subsequent release of CO_2, effectively reversing the CDR benefit of carbonate dissolution.

The exact value of Ωc is site-specific and influenced by nucleation conditions as well as the presence of precipitation inhibitors like Mg^{2+} and phosphates (Morse et al., 2007; Marion et al., 2009). Also dissolved organic matter and related seasonality effects can influence Ωc (Tian et al., 2025). In river systems, Ωc values between 5 and 25 have been suggested (Zhang et al., 2022), although precipitation may occur at lower thresholds depending on local conditions (e.g., Chen et al. (2020)). In this study, we adopt a conservative threshold of Ωc = 2.5 based on the lowest value found in literature (Escoffier et al., 2023; Many et al., 2024) and perform sensitivity analyses for higher values (5, 7.5, and 10).

In simulation 2, we also used the GEMS-GLORI database and PHREEQC and entered initial solutions and pCO_2 in an identical way as in simulation 1. In addition, we added 1 mg $Ca(OH)_2$ per liter through a PHREEQC KINETICS function. The amount of $Ca(OH)_2$ was then iteratively increased until Ω(aragonite) reached Ωc. Aragonite was simulated for precipitation rather than calcite because in seawater aragonite dominates carbonate precipitation (Sun et al., 2015). The same outputs as in Equation 1 were extracted and **Equation 1** was used to determine the gross CDR potential.

2.3 The cost per unit of gross CDR

For every river and application scenario, the cost per unit of gross CDR is the sum of the capital expenditures (CAPEX) and operational expenditures (OPEX) divided by the amount of gross CDR. The OPEX for labor associated with adding lime(stone) to ponds / silos is neglected in this cost estimation. For the OPEX, we considered the cost of limestone, electricity, natural gas and lime(stone) transport (**Equation 2, Table 1**).

$$OPEX\left[\frac{\$}{t\ gross\ CDR}\right] = limestone\ cost + transport\ cost + natural\ gas\ cost + electricity\ cost \qquad \boldsymbol{Eq.2}$$

Table 1: Overview of scenarios and included costs. 1/0 represent whether a cost is in-/excluded in a specific scenario.

	Pond $CaCO_3$	Pond $Ca(OH)_2$	Direct-river $CaCO_3$	Direct-river $Ca(OH)_2$
Scenario	1	2	3	4
Mining+ grinding electricity and diesel	1	1	1	1
Pumping electricity	1	1	0	0
Calcination electricity	0	1	0	1
Natural gas	0	1	0	1

Mining + grinding CAPEX	1	1	1	1
Pond+pump CAPEX	1	1	0	0
Silo CAPEX	0	0	1	1
Sensor CAPEX	1	1	1	1
Calcination CAPEX	0	1	0	1

The cost of limestone was assumed to be 4 \$ t^{-1} (Kowalczyk et al., 2024). For transport costs, we assumed 0.336 and 0.02 \$/ton.km for transportation by truck and sea shipping, respectively (Fan et al., 2018; KiM, 2023). Electricity prices for every country are 2023-25 averages taken from (globalpetrolprices.com, 2025). If available, industrial electricity price averages between 2023-2025 were used. In some cases, these were not available and residential electricity prices were used. Although prices vary regionally (from \$7 MWh^{-1} in the US to \$37 MWh^{-1} in the EU (Hannah Ritchie, Pablo Rosado, 2023)), natural gas was assumed at the 2024 global wholesale price of \$16 MWh^{-1} (International gas union, 2025). We calculated the CAPEX as in **Equation 3**, based on the CAPEX for $CaCO_3$ mining, calcination (if applicable in the scenario) and the cost for the alkalinity addition system. CAPEX was discounted per year as in **Equation 4**.

$$CAPEX\left[\frac{\$}{t\ gross\ CDR}\right] = \frac{[Annualizerd\ Capex\ (pump + pond + EC\ sensor + silo + calcination + mining)]\left[\frac{\$}{installation.year}\right]}{\frac{t\ gross\ CDR}{installation.year}} + \quad (\boldsymbol{Eq.3})$$

Potentially, additional stirring or mechanical agitation may be required, which are not included in these cost estimates (sensitivity analysis, see **supplement Section 4)**. To annualize installation cost, we applied a 5% discount rate and a 15-year lifetime for ponds, pumps and silos. We assume the typical lifetime before desludging wastewater treatment basins as a proxy for ponds (Picot et al., 2004) and a typical lifetime for steel silos (which are affected by corrosion in time) (Sarno et al., 2021))**(Equation 4)**.

$$annualized\ CAPEX\left[\frac{\$}{installation.year}\right] = CAPEX\left[\frac{\$}{installation}\right] * \frac{r*(1+r)^n}{((1+r)^n\ -1\ )}\left[\frac{1}{year}\right] \qquad \boldsymbol{Eq.4}$$

$with\ r = 0.05\ and\ n = 15$

For direct-river application, we assume silos of 80 t limestone capacity, as used before in Scandinavia (Naturvårdsverket, 2011). We estimated the CAPEX of a 80 ton silo to be 3600 \$ (assuming a 45 \$ ton^{-1} silo capacity (COBAN, 2026)) and assumed that a silo is refilled with rocks weekly. As costs of silo foundations, discharge hardware, controls and sensors the real installed cost per silo is likely higher, we conservatively estimated this uncertain CAPEX at 50000\$ per 80 ton silo. For ponds, CAPEX includes construction costs of limestone dissolution ponds, including excavation, pumps and sensors. For excavation, we assumed at 18\$ m^{-3}, the upper estimate for river-widening works (Aerts, 2018). For pumping, a flow rate of 22 $m^3\ s^{-1}$ was deemed sufficient. At this rate, a pond volume

delivering 1 t CDR per batch (maximum 44 161m³, see Table S1, which followed from Simulation 1), could be filled in under 34 minutes. To make eight calcite dissolution batches possible per day, each batch should thus maximally take three hours, which is enough to dissolve $CaCO_3$, assuming a log weathering rate of $10^{-5.8}$ mol m^{-2} s^{-1} (Palandri & Kharaka, 2004). To achieve the required flow, three axial flow pumps are needed with an estimated cost of 1800$ each. The same pump CAPEX was assumed for the $CaCO_3$ and $Ca(OH)_2$ pond scenarios. We assume 800 \$ $year^{-1}$ for MRV costs attributed to EC sensors (2x 400 \$ $sensor^{-1}$). When weighed over the annual amount of CDR estimated per pond (2.9 and 13.1 kton gross CDR per pond for $CaCO_3$ and $Ca(OH)_2$), the cost for one EC sensor adds only 0.01-0.1 \$ t^{-1} gross CDR.

To quantify the gross CDR $installation^{-1}$ $year^{-1}$ a key input is the dissolution time of the rocks. According to Wang et al. (1998), $Ca(OH)_2$ dissolves roughly 100 times faster than $CaCO_3$, enabling dissolution within two minutes. The quantified pump flow rate allows pond filling within 40 minutes – during which $Ca(OH)_2$ is assumed to be dissolved–making 36 pond batches per day possible. The relatively high amount of batches per day substantially reduces CAPEX per unit of CDR [\$ t^{-1} gross CDR]. We assume that ponds are filled and emptied simultaneously after completion of each dissolution batch. The annualized CAPEX for limestone mining and calcination are 1.6 and 14.2 \$ t^{-1} CaO respectively (Kowalczyk et al., 2024). These were converted to \$ t^{-1} gross CDR by multiplying with 0.56 (molar conversion to \$ t^{-1} $CaCO_3$) and with the required t $CaCO_3$ t^{-1} gross CDR (obtained from the PHREEQC simulations).

2.4 Cost per unit of net CDR, Life cycle emissions and Energy needs

To determine the cost per unit of net CDR, we summed OPEX and CAPEX and included life-cycle emissions (**Equation 5)**.

$$net\ CDR\ price\ \left[\frac{\$}{t\ NET\ CDR}\right] = \frac{CAPEX + OPEX\left[\frac{\$}{t\ gross\ CDR}\right]}{\left(\frac{t\ Net\ CDR}{t\ Gross\ CDR}\right)} \qquad \textbf{Eq. 5}$$

The ratio of net/gross CDR cost is calculated by **Equation 6** and depends on the life cycle emissions ($LC_{emissions}$).

$$\left(\frac{Net\ CDR}{Gross\ CDR}\right) = 1 - LC_{emissions}\left[\frac{t\ CO2}{t\ gross\ CDR}\right] \qquad \textbf{Eq. 6}$$

Major Life cycle emissions ($LC_{emissions}$) (**Equation 7**) across different scenarios can result from electricity and fuel consumed for mining and grinding $CaCO_3$, pumping water in ponds, calcination and rock transportation. Mining and grinding $CaCO_3$ rock to a particle size of 100 µm consumes approximately 163.9 MJ/tCaO or 25.5 kwh t^{-1} $CaCO_3$ of electricity (De Marco et al., 2023; Kowalczyk et al., 2024). The carbon intensity of electricity in every river mouth region was sourced from EMBER and electricitymaps.org (Electricitymaps, 2025; EMBER, 2025). In addition, mining and grinding consumes 32.8 MJ t^{-1} CaO or 5 kwh t^{-1} $CaCO_3$ is consumed in the form of diesel with a C intensity of 76 kg CO_2 GJ^{-1} for diesel (Kowalczyk et al., 2024).

$$LC_{emissions}\left[\frac{t\ CO2}{t\ gross\ CDR}\right] = \frac{(mining + grinding + pumping + calcination)_{electricity}\left[\frac{kwh}{t\ rock}\right] * emission\ factor\left[\frac{t\ CO2}{kwh}\right]}{\left[\frac{t\ grossCDR}{t\ rock}\right]} +$$
$$(mining + grinding)_{Diesel} * \left[\frac{kwh}{t\ rock}\right] * emission\ factor\left[\frac{t\ CO2}{kwh}\right] +$$
$$\frac{Transport\ distance[km]}{\left[\frac{t\ grossCDR}{t\ rock}\right]} * emission\ factor\left[\frac{t\ CO2}{t\ rock.km}\right] +$$
$$\left[(nat\ gas)_{\boldsymbol{heat}}\left[\frac{kwh}{t\ gross\ CDR}\right] * emission\ factor\left[\frac{t\ CO2}{kwh}\right] + Chemical\ CaCO3_{decomposition}\left[\frac{t\ CO2}{t\ gross\ CDR}\right]\right] * 0.10$$

Eq. 7

For pond-river RAE, we need to consider emissions related to pumping water to fill or empty ponds. When river water levels are multiple meters below the surrounding land, a vertical lift could be required. In our case, we assumed a pump efficiency of 75% and a 3 m vertical lift. For every river, the water requirement to dissolve $CaCO_3$ (the outcome from PHREEQC simulation 1) was converted into a pumping energy requirement as in **Equation 8.**

$$pumping\ energy\ \left[\frac{kwh}{t\ CaCO_3}\right] = \frac{9.81\frac{N}{kg} * Vertical\ lift\ (m) * 1000\frac{kg}{m^3} * \frac{m^3}{t\ CaCO3}\frac{1\ kwh}{3.6 * 10^6 J}}{pump\ efficiency} \qquad \boldsymbol{Eq.8}$$

For transport, only 30 km of truck transport is assumed, given the abundant limestone reserves in the proximity of ports (Hartmann & Moosdorf, 2012; Phil Renforth et al., 2022). We defined coastal limestone sources as locations with carbonate rock located within 10 km of the coast. While we selected carbonate rock sources located at a maximum of 10 km from the coast, we conservatively assume a land transportation distance of 30 km to also account for potential land transport near the river mouth location. We assume a $CaCO_3$ purity of 98% within limestone, so that the mass of limestone required to be transported is slightly higher than the $CaCO_3$ requirement.

After being transported from the mine to a local port, limestone needs to be shipped to the river mouth. For shipping distances, we determined the shortest shipping distance between the closest coastal $CaCO_3$ formation (derived from the Global Lithological Map Database v1.0, (Hartmann & Moosdorf, 2012)) and each river mouth using the python SEAROUTE package (Pypi.org, 2025). If there was no suitable shipping route from the coastal limestone source to the river mouth (which was the case in 35% of the cases), the shipping distance was approximated by determining the shortest circle distance between mine and river mouth using the distGeo function from the geosphere R package (Hijmans et al., 2024).

For the production of $Ca(OH)_2$, required electricity and natural gas inputs associated with calcination were assumed to be 995 MJ t^{-1} CaO and 3.1 GJ t^{-1}CaO respectively, while a natural gas C intensity of 59 kg CO_2 GJ^{-1} energy was assumed as in Kowalczyk et al. (2024). We assume that 10% of the CO_2 produced during calcination cannot be captured by CCS, as CCS typically achieves C capture rates of 90% (Global CCS institute, 2025).

For direct-river application, we only considered life cycle emissions that are associated with mining, grinding, and transporting limestone. We did not include emissions needed to produce automated lime dosing units that could be placed on the river shore. According to Sterling et al. (2023), particles need to be ground <70 µm to remain in suspension during direct-river application. The additional grinding energy for direct river liming due to grinding finer than 100 µm was estimated with Bonds law (**Equation 9**) with p80 and f80, the particle size larger than 80% of the particles of the grinding product and feed, respectively. A work index (Wi) of 12 kWh t^{-1} was assumed. Calculations indicated that the additional energy needed to grind limestone from 100 to 60 µm - which would be needed to maintain the $CaCO_3$ in suspension during dissolution in direct-river liming (Sterling et al., 2023) - would be negligible (0.349 kWh t^{-1} limestone or about 1 kWh t^{-1} CDR delivered).

$$Grinding\ energy\ \left(\frac{kwh}{tCaCO3}\right) = W_i * \left(\frac{10}{\sqrt{p80}} + \frac{10}{\sqrt{f80}}\right) \qquad \boldsymbol{Eq.9}$$

2.5 Discharge-weighing of variables and further data processing

To ensure representativeness, we calculated discharge-weighted averages for outcome variables (**Equation 10**). Unlike a simple mean, which treats all river systems equally, this method assigns weights proportionally to each river's annual discharge. This prevents low-flow tributaries from disproportionately biasing the results and ensures the final average reflects the true volumetric scale of the total river network.

$$Discharge\ weighed\ water\ requirement\left[\frac{m^3}{t\ rock\ dissolved}\right]$$

$$= \sum_{i=1}^{y} [\left(\frac{\mathrm{m}^3}{t\ rock\ dissolved}\right) river_i * (\frac{annual\ discharge\left(\frac{m^3}{year}\right) river_i}{annual\ discharge\ all\ rivers\ \left(\frac{m^3}{year}\right)})\ ] \quad \boldsymbol{Eq.10}$$

With y as the number of included rivers.

Reported values for water and energy use, as well as costs, the rock mass required per unit of gross CDR and maximum $Ca(OH)_2$ concentration (g L^{-1}) to avoid aragonite precipitation were all weighted by annual river discharge as in **Equation 10**. After the determination of the net CDR potential, rivers with a negative net CDR potential were filtered out of the dataset.

To keep the net CDR cost in range with expected future CO_2 prices across all scenarios (IIASA, 2022), we excluded rivers requiring more than 100,000 $m^3\ t^{-1}$ CDR of dissolution water in this analysis and consider them as too costly due to the high pumping OPEX and pond CAPEX. Since these rivers with high water consumption contributed only a minor share to the total net CDR potential (maximum 7.3% for direct-river $CaCO_3$ and 4.0% for pond-river $CaCO_3$ (η=0.65)), applying this filter did not substantially change the total net CDR potential. For consistency, we also applied the 100000 $m^3\ t^{-1}$ CDR upper boundary filter for RAE with $Ca(OH)_2$, which made a negligible difference as the total net CDR potential with $Ca(OH)_2$ decreased by a maximum of 0.08% across all $Ca(OH)_2$ scenarios.

2.6 Cash-flows: now and under future C prices

Cash flows were estimated based on the cost of net CO_2 removal and CO_2 prices. All data on current CO_2 prices was extracted from ANNEX B in the report of the world bank of 2025 (The World Bank, 2025). We selected the highest CO_2 price if multiple C prices were available (e.g. the EU-ETS price was selected for France as it is higher than the French national C tax). We excluded the USA here due to the lack of a federal C pricing mechanism. Currently, global emissions-weighted average C price is only 5 \$ t^{-1} CO_2 removed (The World Bank, 2025), so that current global economic viability is low. We therefore also quantify cash-flows in 2050, based on the expected CO_2 price (231 \$ t^{-1}) from Integrated Assessment Model scenario EN_NPi2020+F2:Q2_800 (used in the IPCC AR6 Working Group III (IIASA, 2022)). .

3. Results

3.1 Gross and net CDR potential

We quantified the gross and net CDR performance of RAE across 149 of the largest rivers for four implementation scenarios: pond-river and direct-river application of $CaCO_3$ and $Ca(OH)_2$. For RAE using $CaCO_3$, we derived a gross CDR potential between 355-428 Mton CDR $year^{-1}$ (η=0.65-0.85). For RAE using $Ca(OH)_2$ (Ωc=2.5) we derived a gross CDR potential between 1347-1761 Mton CDR $year^{-1}$ (**Figure S2**).

For pond-river RAE, we derived a net CDR potential between 238-339 Mton CDR $year^{-1}$ and between 968-1387 Mton CDR $year^{-1}$ for $CaCO_3$ and $Ca(OH)_2$ respectively (η=0.65-0.85). For direct-river addition of $CaCO_3$ and $Ca(OH)_2$ (Ωc < 2.5), we derived net CDR potentials between 265-378 and 1033-1445 Mton CDR $year^{-1}$ respectively (**Figure 2**). Typically, the ratio of net/gross CDR exceeded 75% for direct-river $CaCO_3$ and $Ca(OH)_2$ addition and was >60% and comparable for pond $CaCO_3$ and $Ca(OH)_2$ applications (**Figure S3**), indicating a substantial life cycle emission penalty of a pond set-up.

3.2 Resource intensity (water, land and energy use)

For the 149 selected undersaturated rivers, we quantify a discharge-weighted water use between 33770-44161 $m^3\ t^{-1}$ gross CDR for $CaCO_3$ across the considered scenarios (**Table S1)**. For $Ca(OH)_2$, less water per unit of CDR is consumed (between 15810-20006 $m^3\ t^{-1}$ gross CDR across different scenarios). This water requirement is equivalent to the pond volume required to deliver a ton CDR and hence the land-use of dissolution ponds. Assuming a 3 m pond depth and gross CO_2 sequestration rates of 2.9 and 13.1 kton CDR $pond^{-1}\ year^{-1}$ for $CaCO_3$ and $Ca(OH)_2$ respectively, the land-use corresponds to 1985-2596 and 19718-24951 t CDR $ha^{-1}\ year^{-1}$ for $CaCO_3$ and $Ca(OH)_2$ respectively.

Another critical resource input is energy. While direct-river RAE using $CaCO_3$ had the lowest energy-use (278-364 kwh t^{-1} CDR, **Table 2**), pond RAE with $Ca(OH)_2$ had the highest energy use (1236-1414 kwh t^{-1} CDR).

3.3 Techno-economic assessment

The discharge-weighed mean cost per unit of net CDR was estimated to be in the range of 241-360, 301-627, 149-208 and 123-194 \$ t^{-1} CDR for pond RAE with $CaCO_3$, pond RAE with $Ca(OH)_2$, direct-river $CaCO_3$ and direct-river $Ca(OH)_2$ application respectively (η = 0.65-0.85) (**Table S1**). Discharge-weighed net CDR costs for direct-river applications were thus substantially lower than those for pond applications. Pond-based applications are more expensive due to the additional CAPEX for ponds (estimated at approximately \$25 per ton of CDR (**Figure 3**)). The higher cost for ponds however primarily stems from the higher OPEX for pumping electricity needed to lift large volumes of water. In ponds, there is a lower pumping electricity demand for $Ca(OH)_2$ relative to $CaCO_3$. Despite the additional electricity and natural gas OPEX for producing $Ca(OH)_2$, the overall costs for RAE with $Ca(OH)_2$ were calculated to be lower than for $CaCO_3$ in ponds due to lower transport and pumping costs (**Figure 3**). The transport OPEX for $Ca(OH)_2$ was lower than transport costs for $CaCO_3$ (**Figure 3**).

Table 2: Estimation of energy use per unit of CDR to dissolve $CaCO_3$ in major rivers. All values are in kWh t^{-1} gross CDR. For all energy uses, the discharge-weighed average was used. Totals for the different scenarios are indicated in bold. Note that discharge-weighted estimates for $CaCO_3$ only include rivers with relatively low water consumption (<100 000 $m^3\ t^{-1}$ CDR) and positive net CDR potentials. Therefore, the amount of rivers included in the discharge-weighted averages differed slightly among scenarios.

Parameter\Rock	$CaCO_3$				$Ca(OH)_2$			
η	0.65	0.85	0.65	0.85	0.65	0.85	0.65	0.85
POND/DIRECT	POND	POND	DIRECT	DIRECT	POND	POND	DIRECT	DIRECT
Number of included rivers in this analysis	79	80	80	87	134	140	138	140
Calcination electricity + heat (natural gas)	/	/	/	/	234 + 874	201 + 748	264 + 982	201 + 748
Mining + Grinding to 100 µm (electricity + diesel)	93+18	71+14	93+18	73+14	46+9	40+8	51+10	40+8

Pumping electricity (3m lift)	479	368	/	/	174	172	/	/
transport Truck + shipping	252	193	253	191	77	68	89	68
Total	**842**	**646**	**364**	**278**	**1414**	**1236**	**1397**	**1064**

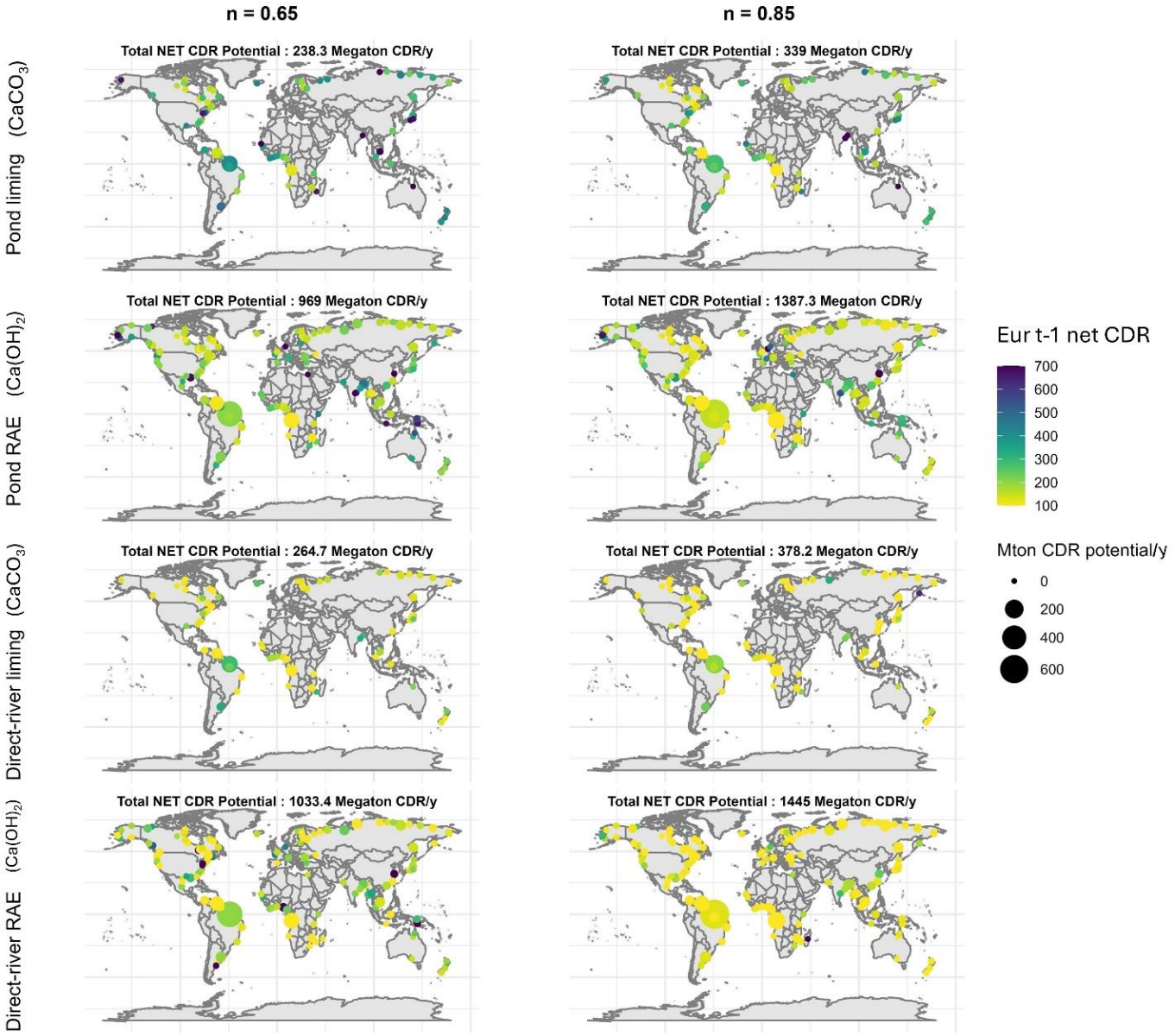

Figure 2: Net CDR potential and the estimated cost for net CDR for large rivers accounting for 55% of the global fresh water discharge to the oceans for pond- and direct-river liming and direct-river $Ca(OH)_2$ addition. For RAE using $Ca(OH)_2$, a conservative Ωc threshold of 2.5 was assumed. In the left and right column of plots, alkalinization efficiencies of 65 and 85% were assumed, respectively.

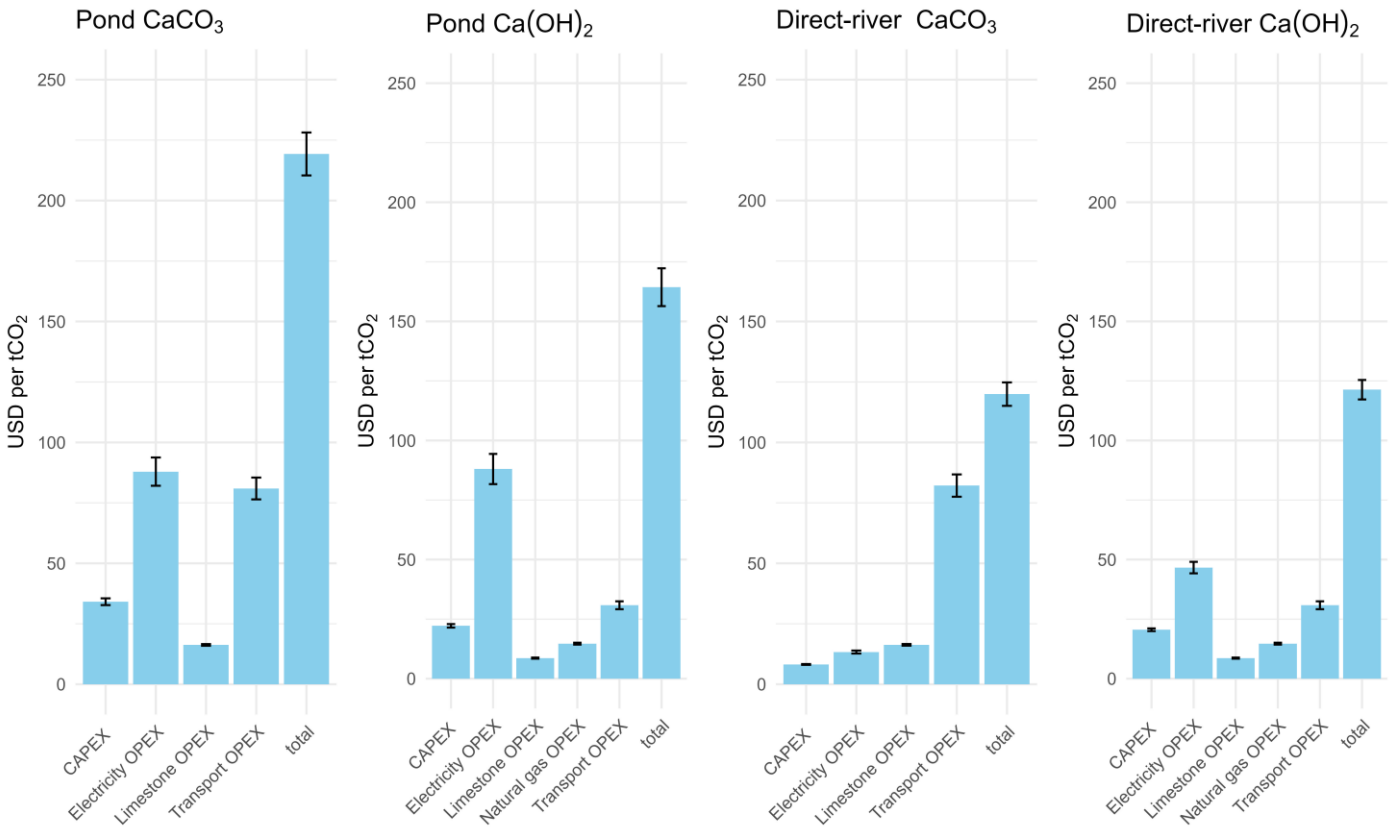

Figure 3: CAPEX and OPEX contributors of the cost per unit of gross CDR. Bar heights and error bars represent the mean ± standard error of all investigated rivers with a positive net CDR potential and a water consumption < 100 000 m^3 t^{-1} CDR. For this figure, η = 0.65 was assumed.

4. Discussion

4.1 CDR potential

While our quantified net CDR potential for the selection of 149 large rivers is substantial (>200, but <400 Mton across all $CaCO_3$ scenarios) and RAE with $CaCO_3$ could deliver some 'low-hanging fruit oppertunities' from an energy input perspective (**Table 2**), our analysis indicates that reaching gigaton scale CDR with river liming is unlikely to be achieved.

In contrast, gigaton scale net CDR could be reached with $Ca(OH)_2$, even with the conservative Ωc=2.5 assumed here. A sensitivity analysis across different values for Ωc (up to 10) indicated that in the case of Ωc = 10, gross CDR potential for RAE with $Ca(OH)_2$ in the selected rivers may even exceed 3 Gton CDR $year^{-1}$ (**Table S2).**

4.2 Resource intensity (water, land and energy)

In pond applications, substantial amounts of fresh water are pumped for rock dissolution, after rock dissolution, water is discharged back into rivers and is thus not actually consumed. However, there is additional land-use required in pond approaches, which is not required in the direct-river application. The estimated C sequestration per unit of land use for ponds used for $CaCO_3$ and $Ca(OH)_2$ dissolution, respectively, was 1985-2596 and 19718-24951 tCO_2 ha^{-1} $year^{-1}$. For comparison, forests typically sequester CO_2 at roughly 11-13 tCO_2 ha^{-1} yr^{-1} (Cook-Patton et al., 2020; Griscom et al., 2017). Despite the orders of magnitude higher per-area CDR efficiency of ponds relative to forests, ponds can only be established in limited areas near rivers. Forests, on the other hand, can be planted in a wider range of locations and offer additional benefits beyond carbon sequestration, such as supporting biodiversity. Direct river liming with $CaCO_3$ or $Ca(OH)_2$ would require no additional land aside from land used to place automated lime spreaders along the shore.

The estimated energy use for RAE compares favorably to other CDR approaches (**Figure S7**). Most established DACCS systems typically have an energy footprint of approximately at 2000 kwh t^{-1} CDR (McQueen et al., 2021). Some geochemical CDR methods can demand more energy, like electrochemical olivine upgrading to $Mg(OH)_2$ at 2268 kWh t^{-1} CDR without a CO_2 point source (Scott et al., 2021). However, typically, geochemical CDR methodologies have lower energy demands than DACCS. The energy requirement for ocean liming for example ranges between 1333-2000 kWh t^{-1} CDR (Kowalczyk et al., 2024). The latter energy consumption for ocean liming includes diesel consumed to spread $Ca(OH)_2$ offshore, a necessary practice to avoid local oversaturation and reversal of CDR. Using a RAE approach with automated $CaOH_2$ dosing units rather than ships to gradually add $Ca(OH)_2$ may save substantial quantities of diesel relative to ocean liming (**Figure 4).** Replacing DACCS or ocean liming with RAE that dissolves $CaCO_3$ in undersaturated rivers could save even more energy per unit of CDR (**Figure 4**). If the full potential for direct-river $CaCO_3$ in our considered rivers would be realized, energy savings would range between 59-115 and 39-91 GW relative to scenarios where CDR is realized with DACCS or ocean liming respectively (**Figure 4**). In conclusion, river liming may be low-hanging fruit for CDR, consuming a relatively limited amount of energy, especially if $CaCO_3$ is used.

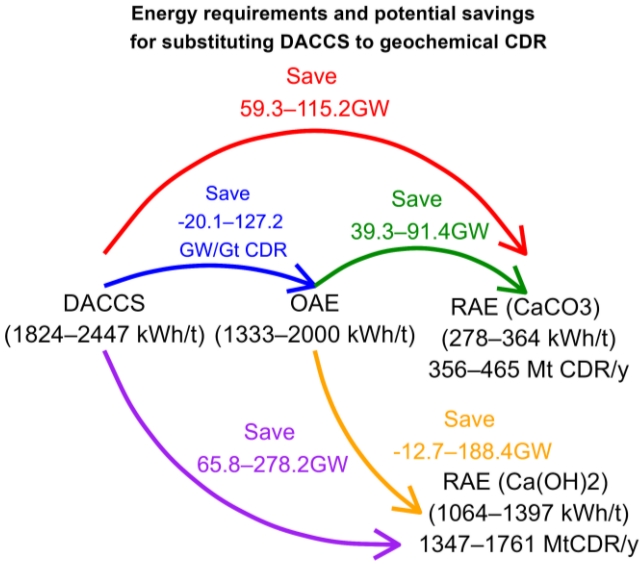

Figure 4: Theoretical energy savings of replacing more energy intensive forms of CDR with RAE, assuming the maximum RAE CDR potential is realized. Direct-river application of $CaCO_3$ and $Ca(OH)_2$ were assumed for RAE in this figure. Energy consumptions of different CDR technologies were sourced from the references cited in the paragraphs above this figure. Potential energy savings for RAE represent the maximum possible energy savings in the considered large rivers in this study. Theoretically, multiple Gtons of DACCS could be replaced by ocean liming, therefore potential energy savings of this transition are expressed per Gton of CDR replacement.

RAE can achieve similar or lower energy use per unit of CDR than terrestrial EW, particularly when EW requires substantial land transport of rock materials. Assuming 18.9 kWh t^{-1} for basalt comminution to <100 µm (Rinder & von Hagke, 2021) a CDR efficiency of 0.23 tCO_2 t^{-1} basalt (Lefebvre et al., 2019) and a transport energy of 0.61 kWh t^{-1} transported km^{-1} by truck, the energy consumption of terrestrial EW equals that of direct-river $CaCO_3$ addition after 69–99 km of transport. However, an inorganic CO_2 removal with an efficiency of 0.23 tCDR t^{-1} basalt has not been achieved yet in practice, likely due to cation retention in top soils delaying CDR realization (Steinwidder et al., 2025). The energy consumption of RAE with $Ca(OH)_2$ however, could be up to about 1000 kwh t^{-1} CDR higher than in terrestrial EW (**Figure S7)**.

4.3 Techno-economic assessment

Costs for CDR using $Ca(OH)_2$ are generally comparable to those with $CaCO_3$, despite the higher energy inputs associated with $Ca(OH)_2$ production (**Table 2**). As we explicitly assumed that calcination occurs before transport, transport costs are lower for $Ca(OH)_2$ than for $CaCO_3$, due to its lower molecular weight. In addition, while calcination requires natural gas and electricity (**Figure 3**), $Ca(OH)_2$ dissolves quicker than $CaCO_3$ and needs less water, pumping energy and smaller pond sizes, reducing both CAPEX and operational electricity costs (**Table S1, Figure 4)**.

Direct-river applications could deliver CDR costs around or below $200 per ton net CDR, whereas pond-based methods tend to be more expensive (**Figure S4**). Although ponds incur higher CAPEX and operational expenses, they offer enhanced measurability and control in a closed system. This additional investment could be avoided by utilizing existing infrastructure such as wastewater treatment plants or dams. Potentially, multi-purpose basins that are e.g. also used for aquaculture or pumped hydro energy storage could be used. Our assessment excludes energy recovery from gravitational water flow from ponds back to rivers. While pond-based RAE provides better monitoring capabilities and could be used to calibrate models in specific river sections, ponds demands more financial, energy and land resources than direct-river approaches. If future research confirms efficient rock dissolution and reliable CDR measurement in rivers, dedicated pond infrastructure may be unnecessary, allowing direct-river RAE to substantially lower costs by eliminating pond-related expenses.

The net CDR cost of RAE may be competitive with DACCS (currently typically sold at ~$490 tCO_2^{-1}) but remains higher than biochar which breakeven at ~$140 tCO_2^{-1} (CDR.FYI, 2025). The discharge-weighed average cost for net CO_2 removal for RAE is higher than the 2026 global emission-weighed CO_2 price (5 $ t^{-1} CO_2). Currently, RAE would thus not be profitable on governmental C markets. Nonetheless, in countries with the highest CO_2 prices and low removal costs, RAE could already breakeven today (**Figure S4, η =0.85)**. For example, direct-river $Ca(OH)_2$ addition (η=0.85) in the Uruguay (Uruguay) and Luleälven (Sweden) rivers was calculated to cost 124 and 72 $ t^{-1} CDR respectively, lower than the national CO_2 prices of 158.8 and 144.6 $ t^{-1} CO_2 respectively. Also for the Ebro (Spain) and the Seine (France) we calculated a positive cash flow today for direct-river $Ca(OH)_2$ due to relatively cheap, low-C intensive energy and proximity of carbonate lithology delivering limited transport costs. Direct-river $CaCO_3$ addition would also break-even in several Canadian rivers under current ETS prices (**Figure S4**). For pond $CaCO_3$ RAE, negative cash flows would be generated for every river in 2026. If the expected 2050 CO_2 price (231 $ t^{-1} CO_2) would apply globally, positive cash flows would be generated in most of the assessed rivers, across all four considered scenarios (**Figure S5**).

4.4 Risks (and co-benefits)

An important risk associated with RAE is reversibility of CDR, while both risks and co-benefits may arise from increased pH or TA in rivers. In addition, potential environmental impacts as well as incomplete riverine mineral dissolution should be considered.

Reversibility of CDR arises when CO_2 sequestered during rock dissolution is released again through downstream carbonate precipitation (**Table S3**). Nonetheless, reversibility of CDR is not expected to be a concern for RAE via river liming with $CaCO_3$ (**Figure 5**), because this is applied only in rivers where calcite saturation is below equilibrium ($\Omega < 1$), preventing $CaCO_3$ precipitation. The amount of water required to undersaturate $CaCO_3$ can be lower when a CO_2 point source is present, a focus of study in a CCS strategy named accelerated weathering of limestone (AWL) (Huysmans et al., 2025).

If river water is oversaturated with respect to $CaCO_3$ ($\Omega >1$), it is still possible to realize CDR by applying carbonate-derivatives such as $Ca(OH)_2$. Carbonate-derivatives and silicates can dissolve in waters where $\Omega > 1$, albeit with a risk of losing up to 50% of the initially captured CDR if $\Omega > \Omega c$. When no external CO_2 source is present silicates however dissolve too slowly to provide meaningful C sequestration within years ($\log Wr < -12$, (Amann et al., 2022)) such that a point source of CO_2 emissions is required for silicates.

To prevent reversibility and CO_2 losses, rivers with a $\Omega<\Omega c$ should be selected for RAE. If Ωc is exceeded, 'runaway precipitation' – due to which significantly more alkalinity is removed than was initially added- could take place (Moras et al., 2022), so that RAE is not recommended in such situations. If $\Omega > \Omega c$, RAE with $CaCO_3$ may not deliver CDR, as downstream carbonate precipitation could release CO_2 again. A question remains what the Ωc for specific rivers is, which is still poorly understood and needs further investigation. For every river where RAE is adopted, Ωc should be determined experimentally across seasons as pioneered in the Elbe (Tian et al., 2025).

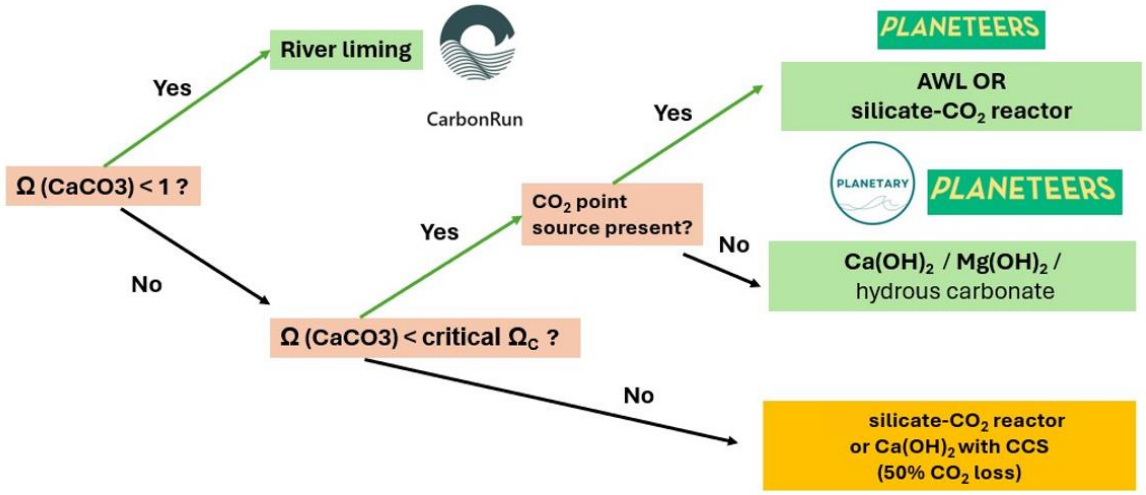

Figure 5: A conservative workflow to avoid reversibility issues in RAE: based on the saturation of $CaCO_3$ in the river rock feedstock to use for RAE could be selected. Logos of specific RAE start-ups, exploring specific strategies were added for each pathway. AWL = Accelerated weathering of limestone. Ωc=critical saturation state of $CaCO_3$ whereby precipitation initiates. CCS= Carbon capture and storage. When Ω exceeds Ωc (the bottom right case, orange box), RAE is not recommended due to the risk of runaway precipitation.

Environmental risks of RAE include effects on aquatic life, stimulation of microbial metabolism and potential impacts on photosynthesis. The increase of river pH after discharge of the limed water could negatively impact aquatic organisms that prefer acidic conditions. On the other hand, organisms suffering from ocean acidification could benefit from this river liming intervention. In acidified waters, increasing freshwater pH to a more neutral pH can be a co-benefit. River liming was historically applied to alleviate acid stress and improve productivity for species sensitive to acidic waters, such as Atlantic salmon (Sterling et al., 2023). Synergies between CDR and (existing) aquaculture infrastructure may therefore exist. A systematic review of 47 studies found that freshwater liming in acidified Nordic rivers and lakes was generally associated with increased overall fish abundance, with salmon populations benefiting more than brown trout, while no consistent effect was observed on invertebrate abundance (Mant et al., 2013). It needs to be emphasized that rivers in the latter review had a pre-treatment pH of approximately 5, which increased to about 6 after liming.

In our analysis, liming with $CaCO_3$ increased river pH on average with 0.71 units and remained below pH 8.25 for all cases (**Figure S6**). Our pre-treatment pH already ranged between 6.4-7.8, which is increased to between 7.5-8.25 after adding $CaCO_3$ and to between 7.7-8.4 when adding $Ca(OH)_2$ up to Ωc. In essence, the envisioned RAE intervention does not compensate for acidity caused by e.g. sulphur pollution as has been done in nordic rivers historically but changes the state of rivers from a neutral to a slightly-moderately alkaline system. The substantial dilution required to dissolve limestone (tens of thousands $m^3\ t^{-1}$ CDR) limits river water pH increases to 8.25. Still, this is a considerable pH increase, yet the ranges reported in this paragraph are only realized when the upper limit of CDR would be realized for these rivers. Future river-specific risk assessments should estimate how much of the geochemical CDR potential of river liming may actually be safely realized in these rivers.

Similar as in terrestrial enhanced weathering (EW) (Yan et al., 2023), an increase in river pH could also boost riverine microbial activity, provided that the optimal pH for decomposition exceeds the river's initial pH. Not only DOC in rivers may be impacted, flooding of more alkaline water on river adjacent peatlands could also increase pH there and stimulate microbial peat metabolization. If this risk proves to be relevant, avoiding such environments downstream from the river liming operation could mitigate this risk.

Thirdly, excessive riverine TA increases could alter photosynthesis by aquatic plants. Sterling et al. (2023) argue that river liming should be constrained to a maximum of 0.6 mM TA in low-alkalinity rivers, to avoid disruptive shifts in photosynthesis. At elevated TA, freshwater plants are more likely to use bicarbonate (HCO_3^-) instead of dissolved CO_2 for photosynthesis, which could lead to a shift in primary producer communities from CO_2-users to HCO_3^--users (Iversen et al., 2019). Photosynthesis may also be stimulated as liming aquaculture ponds has been shown to decrease water turbidity, increasing the penetration of light and facilitating photosynthesis (Chanda et al., 2019). If river liming reduces turbidity, the resulting increase in light penetration could stimulate growth of aquatic plants — light is a major limiting factor for submerged aquatic vegetation (Hussner et al., 2010) — representing an additional pathway by which liming may contribute to atmospheric CO_2 drawdown.

A last risk and key consideration is incomplete riverine mineral dissolution. Effective application of RAE requires balancing two constraints: ensuring full mineral dissolution before ocean entry and minimizing interference with existing freshwater ecosystems. First, $CaCO_3$ must dissolve entirely within the river system, since seawater is already oversaturated with respect to $CaCO_3$. This requirement sets a minimum upstream distance for the application. For example, if finely ground limestone dissolves in ~2.4 hours and the Amazon River flows at ~5 km h^{-1}, application must occur at least 12 km upstream to ensure complete dissolution. Minerals with slower dissolution kinetics, such as olivine, are unsuitable in this context: with dissolution rates at neutral pH roughly five orders of magnitude lower than calcite (Palandri & Kharaka, 2004), only negligible amounts would dissolve before reaching the ocean (Rønning, 2024).

Simultaneously application should not occur too far upstream (e.g. smaller tropical streams with acidic blackwaters and acidophilic species should be avoided to prevent ecological risks and more rapid organic matter metabolization by microbes) and downstream to avoid incomplete dissolution. As the post-application pHs in our simulation approach the pH of seawater, application could take place as close as possible to the ocean to minimize disturbance of natural systems. Applying RAE in a zone of e.g. several tens of kms near river mouths or estuaries, therefore, may compromise achieving complete dissolution while avoiding substantial ecological risks.

4.5 Practical constraints

When exploring the idea of RAE, practical constraints about spatial application, mixing and EC signal detectability arose. Our CDR estimates assume treatment of 100% of river discharge, representing an upper bound rather than a realistic scenario.

Our simulations assume a single-river extraction location with uniform background chemistry. In reality, RAE deployment would likely be spatially distributed along river reaches, leading to progressive chemical modification of water by upstream dissolution processes. Such spatial feedback could gradually increase alkalinity and cation concentrations downstream, increasing water volume requirements per ton of CDR and associated pond CAPEX and pumping OPEX. For direct-river RAE, we do not anticipate a substantial effect from the "single-extraction" assumption as there is no pond CAPEX and pumping OPEX. In conclusion, as more RAE is applied in a river and background TA increases, pond-based RAE applications are expected to become less attractive, making direct-river RAE an increasingly preferable option (**Supplement, section 5**).

We also evaluated the assumption that mixing is not required (**Supplement, section 4).** 60 µm $CaCO_3$ particles are estimated to settle within 15 minutes in a 3 meter depth pond, so mixing is needed to keep them suspended after initial turbulence. However, $Ca(OH)_2$ dissolves faster and is not

expected to settle before fully dissolving. Mixing was estimate to require about 0.5 W/m³, adding roughly 7% to the process energy. Installation costs for mixers are expected to be minor compared to overall pond expenses, making this a manageable addition.

Another practical constraint may be the detectability of EC increases in large volumes of water where the EC signal may be dwarfed by background EC and could hence not be detectable (see **Supplement, section 7).** The accuracy of such EC sensors (typically 3%) should be sufficient to detect the signal from rock dissolution in ponds. For direct-river application however, detection of the EC signal depends on the amount of rock that is applied and the water flux of the river.

4.6 Commercial interest

Although research on RAE remains limited, commercial interest has grown in recent years, prompting the development of an MRV standard for CDR via RAE (Isometric, 2025). The company 'Carbonrun' aims to apply direct-river liming, while other companies are currently exploring RAE in more controlled environments. Wastewater alkalinity enhancement is already commercially exploited by the companies 'CREW Carbon' (focusing on $CaCO_3$ dissolution during primary wastewater treatment) and 'Planetary' ($Mg(OH)_2$ addition to WWTP effluent).

RAE in existing WWTP flows could be an attractive pathway as controlled systems can be implemented without additional CAPEX or OPEX, allowing costs that may be similar to direct-river RAE. In addition, the elevated pCO_2 due to oxidation of organic matter in WWTPs decreases the water needed for carbonate dissolution. CREW carbon, the CDR start-up aiming to sequester CO_2 by liming in WWTPs reported an 18 million gallon per day facility and an annually achieved CO_2 removal capacity of 2000 tons (equivalent to 12400 $m^3\ t^{-1}$ CDR (CREW CARBON, 2025)).

Nonetheless, the global CDR potential of RAE using WWTPs alone is relatively modest. Even when all global WWTP effluents (estimated at 359.10^9 m^3/year) (Jones et al., 2021) would be supplied with $CaCO_3$, the global potential would be limited at roughly 29 Mton CDR $year^{-1}$. In conclusion, to further increase the global CDR potential of RAE through liming, more water is needed than WWTP effluent alone. The addition of carbonate-derivatives such as $Ca(OH)_2$ in WWTPs could increase the global CDR potential of RAE in WWTPs, yet requires more energy.

5. Conclusions

Reducing the impact of climate change to a minimum will require gigaton-scale CDR solutions that are both scalable and verifiable. This study investigated the technical, energy, economic, and ecological aspects of river alkalinity enhancement (RAE), examining four approaches (pond- and direct-river application of $CaCO_3$ and $Ca(OH)_2$) across 149 of the largest rivers globally, representing 55% of global runoff to oceans. We find that RAE in the studied rivers can deliver substantial net CDR, with an estimated upper limit > 200 but <400 Mt CDR yr^{-1} for $CaCO_3$ and >1 $GtCO_2\ yr^{-1}$ for $Ca(OH)_2$, even under conservative $CaCO_3$ reprecipitation assumptions (Ωc = 2.5) and after subtraction of major life cycle emissions.

In addition, RAE is identified as an attractive CDR technology given the relatively low land- and energy use required for CDR relative to other (geochemical) CDR options. Especially direct-river RAE with $CaCO_3$ in undersaturated rivers may be low-hanging fruit for CDR, consuming limited amounts of energy. For RAE, $Ca(OH)_2$ offers the highest CDR potential and smaller land and water requirements, albeit at the expense of additional required calcination energy and the need for CCS.

The cost of CDR through RAE may be below 200$ $t^{-1}CO_2$, which compares favorably relative to other CDR technologies that do not rely on photosynthesis. Surprisingly, our cost analysis indicates that RAE with $Ca(OH)_2$ is not necessarily more expensive than RAE with $CaCO_3$, if calcination occurs before transportation of $CaCO_3$. Today, RAE could theoretically already be economically viable in specific regions with high CO_2 prices, local carbonate rock and low energy costs. Nonetheless, societal CO_2

prices should rise substantially to allow for positive cash-flows and hence widespread RAE adoption. Before widespread RAE adoption can occur, we argue that potential risks such as reversal of CDR, ecological impacts and practical RAE application strategies should be thoroughly studied. Commercial interest is emerging and existing infrastructure such as WWTPs can play a role in early deployment, although their global potential is limited relative to the gigaton-scale opportunities in natural rivers.

In summary, RAE emerges as a promising addition to the geochemical CDR portfolio: scalable, relatively energy-efficient and compatible with tightly monitored, sensor-based MRV if closed dissolution systems are used. Achieving its potential will require further experimental validation of dissolution dynamics and careful river-specific assessments of saturation thresholds and ecological risks. As part of a diversified climate change mitigation portfolio, RAE could complement existing CDR approaches and help bridge the gap to gigaton-scale removals needed for limiting warming below 2 °C.

References

Aerts, J. C. J. H. (2018). A review of cost estimates for flood adaptation. Water, 10(11), 1646. https://doi.org/10.3390/w10111646

Amann, T., & Hartmann, J. (2022). Carbon accounting for enhanced weathering. Frontiers in Climate, 4, 849948. https://doi.org/10.3389/fclim.2022.849948

Amann, T., Hartmann, J., Hellmann, R., Pedrosa, E. T., & Malik, A. (2022). Enhanced weathering potentials—the role of in situ CO2 and grain size distribution. Frontiers in Climate, 4, 929268. https://doi.org/10.3389/fclim.2022.929268

Batchelor-McAuley, C., Yang, M., Rickaby, R. E. M., & Compton, R. G. (2022). Calcium Carbonate Dissolution from the Laboratory to the Ocean: Kinetics and Mechanism. Chemistry - A European Journal, 28(68). https://doi.org/10.1002/chem.202202290

Cai, W. J., & Jiao, N. (2022). Wastewater alkalinity addition as a novel approach for ocean negative carbon emissions. Innovation, 3(4), 100272. https://doi.org/10.1016/j.xinn.2022.100272

CARBON, C. (2025). CREW carbon. https://crewcarbon.com/projects/

Caserini, S., Storni, N., & Grosso, M. (2022). The Availability of Limestone and Other Raw Materials for Ocean Alkalinity Enhancement. Global Biogeochemical Cycles, 36(5). https://doi.org/10.1029/2021GB007246

Chen, B. B., Li, S. L., Pogge von Strandmann, P. A. E., Sun, J., Zhong, J., Li, C., Ma, T. T., Xu, S., & Liu, C. Q. (2020). Ca isotope constraints on chemical weathering processes: Evidence from headwater in the Changjiang River, China. Chemical Geology, 531, 119341. https://doi.org/10.1016/j.chemgeo.2019.119341

Clarkson, M. O., Larkin, C. S., Swoboda, P., Reershemius, T., Suhrhoff, T. J., Maesano, C. N., & Campbell, J. S. (2024). A review of measurement for quantification of carbon dioxide removal by enhanced weathering in soil. Frontiers in Climate, 6, 1345224. https://doi.org/10.3389/fclim.2024.1345224

COBAN. (2026). how much does a silo cost? https://kbsilo.com/how-much-does-a-silo-cost

Cook-Patton, S. C., Leavitt, S. M., Gibbs, D., Harris, N. L., Lister, K., Anderson-Teixeira, K. J., Briggs, R. D., Chazdon, R. L., Crowther, T. W., Ellis, P. W., Griscom, H. P., Herrmann, V., Holl, K. D., Houghton, R. A., Larrosa, C., Lomax, G., Lucas, R., Madsen, P., Malhi, Y., Paquette, A., Parker, J. D., Paul, K., Routh, D., Roxburgh, S., Saatchi, S., van den Hoogen, J., Walker, W. S., Wheeler, C. E., Wood, S. A., Xu, L., & Griscom, B. W. (2020). Mapping carbon accumulation potential from global natural forest regrowth. Nature, 585, 545–550. https://doi.org/10.1038/s41586-020-2686-x

De Marco, S., Varliero, S., Caserini, S., Cappello, G., Raos, G., Campo, F., & Grosso, M. (2023). Techno-economic evaluation of buffered accelerated weathering of limestone as a CO2 capture and storage option. Mitigation and Adaptation Strategies for Global Change, 28(3). https://doi.org/10.1007/s11027-023-10052-x

Dupla, X., Möller, B., & Baveye, P. C. (2023). Potential accumulation of toxic trace elements in soils during enhanced rock weathering. European Journal of Soil Science, 74(1), e13343. https://doi.org/10.1111/ejss.13343

Electricitymaps. (2025). Electricitymaps. https://app.electricitymaps.com/

EMBER. (2025). EMBER. https://ember-energy.org/data/electricity-data-explorer/

Escoffier, N., Perolo, P., Many, G., Pasche, N. T., & Perga, M. E. (2023). Fine-scale dynamics of calcite precipitation in a large hardwater lake. Science of the Total Environment, 864, 160699. https://doi.org/10.1016/j.scitotenv.2022.160699

Fan, Y. Van, Perry, S., Klemeš, J. J., & Lee, C. T. (2018). A review on air emissions assessment: Transportation. Journal of Cleaner Production, 194, 673–684. https://doi.org/10.1016/j.jclepro.2018.05.151

Fekete, B. M., Vörösmarty, C. J., & Grabs, W. (2002). High-resolution fields of global runoff combining observed river discharge and simulated water balances. Global Biogeochemical Cycles, 16(3), 15-1-15–10. https://doi.org/10.1029/1999gb001254

Flipkens, G., Blust, R., & Town, R. M. (2021). Deriving Nickel (Ni(II)) and Chromium (Cr(III)) Based Environmentally Safe Olivine Guidelines for Coastal Enhanced Silicate Weathering. Environmental Science and Technology, 55(18), 12362–12371. https://doi.org/10.1021/acs.est.1c02974

Geerts, L. J. J., Hylén, A., & Meysman, F. J. R. (2025). Review and syntheses: Ocean alkalinity enhancement and carbon dioxide removal through coastal enhanced silicate weathering with olivine. Biogeosciences, 22(2), 355–384. https://doi.org/10.5194/bg-22-355-2025

Global CCS Institute. (2025). Advancements in CCS technologies and costs. Global CCS Institute. https://www.globalccsinstitute.com/wp-content/uploads/2025/08/Advancements-in-CCS-Technologies-and-Costs-Report-2.pdf

Globalpetrolprices.com. (2025). Electricity prices. Retrieved September 30, 2025, from https://www.globalpetrolprices.com/electricity_prices/

Griscom, B. W., Adams, J., Ellis, P. W., Houghton, R. A., Lomax, G., Miteva, D. A., Schlesinger, W. H., Shoch, D., Siikamäki, J. V., Smith, P., Woodbury, P., Zganjar, C., Blackman, A., Campari, J., Conant, R. T., Delgado, C., Elias, P., Gopalakrishna, T., Hamsik, M. R., Herrero, M., Kiesecker, J., Landis, E., Laestadius, L., Leavitt, S. M., Minnemeyer, S., Polasky, S., Potapov, P., Putz, F. E., Sanderman, J., Silvius, M., Wollenberg, E., & Fargione, J. (2017). Natural climate solutions. Proceedings of the National Academy of Sciences, 114(44), 11645–11650. https://doi.org/10.1073/pnas.1710465114

Ritchie, H., Rosado, P., & Roser, M. (2023). Natural gas prices. Our World in Data. https://archive.ourworldindata.org/20250909-093708/grapher/natural-gas-prices.html

Hartmann, J., & Moosdorf, N. (2012). The new global lithological map database GLiM: A representation of rock properties at the Earth surface. Geochemistry, Geophysics, Geosystems, 13(12). https://doi.org/10.1029/2012GC004370

Hijmans, R. J., Karney, C., Williams, E., & Vennes, C. (2024). geosphere: Spherical trigonometry (R package). https://cran.r-project.org/web/packages/geosphere/index.html

Hussner, A., Hoelken, H. P., & Jahns, P. (2010). Low light acclimated submerged freshwater plants show a pronounced sensitivity to increasing irradiances. Aquatic Botany , 93 (1), 17–24.https://doi.org/10.1016/j.aquabot.2010.02.003

Huysmans, T., Meysman, F. J. R., & Van De Velde, S. J. (2025). Reviews and syntheses: Potential and limitations of oceanic carbon dioxide storage via reactor-based accelerated weathering of limestone. Biogeosciences, 22(20),5557-5572. https://doi.org/10.5194/bg-22-5557-2025

IIASA. (2022). AR6 scenarios database. https://doi.org/10.5281/zenodo.5886911

International gas union. (2025). Wholesale Gas Price Survey 2025 Edition. https://www.igu.org/press-releases/2025-wholesale-gas-price-survey

IPCC. (2023). Summary for Policymakers of the Intergovernmental Panel on Climate Change. Climate Change 2023: Synthesis Report. Contribution of Working Groups I, II and III to the Sixth Assessment Report of the Intergovernmental Panel on Climate Change, pp. 1-34. https://doi.org/10.59327/IPCC/AR6-9789291691647.001

Isometric. (2025). Isometric protocol for RAE. https://registry.isometric.com/protocol/river-alkalinity-enhancement/1.0/ctn_1JQ8ZCFJY1S0ZWXH#reporting-of-uncertainty

Iversen, L. L., Winkel, A., Baastrup-Spohr, L., Hinke, A. B., Alahuhta, J., Baattrup-Pedersen, A., Birk, S., Brodersen, P., Chambers, P. A., Ecke, F., Feldmann, T., Gebler, D., Heino, J., Jespersen, T. S., Moe, S. J., Riis, T., Sass, L., Vestergaard, O., Maberly, S. C., Sand-Jensen, K., & Pedersen, O. (2019). Catchment properties and the photosynthetic trait composition of freshwater plant communities. Science, 366(6467), 878–881. https://doi.org/10.1126/science.aay5945

Jones, E. R., Van Vliet, M. T. H., Qadir, M., & Bierkens, M. F. P. (2021). Country-level and gridded estimates of wastewater production, collection, treatment and reuse. Earth System Science Data, 13(2), 237–254. https://doi.org/10.5194/essd-13-237-2021

Kanzaki, Y., Planavsky, N. J., Zhang, S., Jordan, J., Suhrhoff, T. J., & Reinhard, C. T. (2025). Soil cation storage is a key control on the carbon removal dynamics of enhanced weathering. Environmental Research Letters, 20, 074055. https://doi.org/10.1088/1748-9326/ade0d5

Kowalczyk, K. A., Amann, T., Strefler, J., Vorrath, M. E., Hartmann, J., De Marco, S., Renforth, P., & Foteinis, S. (2024). Marine carbon dioxide removal by alkalinization should no longer be overlooked. Environmental Research Letters, 19(7), 011003. https://doi.org/10.1088/1748-9326/ad5192

Keith, D. W., Holmes, G., St. Angelo, D., & Heidel, K. (2018). A Process for Capturing CO2 from the Atmosphere. Joule, 2(8), 1573–1594. https://doi.org/10.1016/j.joule.2018.05.006

Kelemen, P. B., McQueen, N., Wilcox, J., Renforth, P., Dipple, G., & Vankeuren, A. P. (2020). Engineered carbon mineralization in ultramafic rocks for CO2 removal from air: Review and new insights. Chemical Geology, 550, 119628. https://doi.org/10.1016/j.chemgeo.2020.119628

Kelland, M. E., Wade, P. W., Lewis, A. L., Taylor, L. L., Sarkar, B., Andrews, M. G., Lomas, M. R., Cotton, T. E. A., Kemp, S. J., James, R. H., Pearce, C. R., Hartley, S. E., Hodson, M. E., Leake, J. R., Banwart, S. A., & Beerling, D. J. (2020). Increased yield and CO2 sequestration potential with the C4 cereal Sorghum bicolor cultivated in basaltic rock dust-amended agricultural soil. Global Change Biology, 26(6), 3658–3676. https://doi.org/10.1111/gcb.15089

KiM. (2023). Cost Figures for Freight Transport - final report. https://www.kimnet.nl/site/binaries/site-content/collections/documents/2023/03/30/kostenkengetallen-voor-het-goederenvervoer/Cost%2Bfigures%2Bfor%2Bfreight%2Btransport_def.pdf

Klemme, A., Rixen, T., Müller, M., Notholt, J., & Warneke, T. (2022). Destabilization of carbon in tropical peatlands by enhanced weathering. Communications Earth & Environment, 3, 212. https://doi.org/10.1038/s43247-022-00544-0

Knapp, W. J., & Tipper, E. T. (2022). The efficacy of enhancing carbonate weathering for carbon dioxide sequestration. Frontiers in Climate, 4. https://doi.org/10.3389/fclim.2022.928215

Köhler, P., Hartmann, J., & Wolf-Gladrow, D. A. (2010). Geoengineering potential of artificially enhanced silicate weathering of olivine. Proceedings of the National Academy of Sciences of the United States of America, 107(47), 20228–20233. https://doi.org/10.1073/pnas.1000545107

Kowalczyk, K. A., Amann, T., Strefler, J., Vorrath, M. E., Hartmann, J., De Marco, S., Renforth, P., Foteinis, S., & Kriegler, E. (2024). SI: Marine carbon dioxide removal by alkalinization should no longer be overlooked. Environmental Research Letters, 19(7). https://doi.org/10.1088/1748-9326/ad5192

Lefebvre, D., Goglio, P., Williams, A., Manning, D. A. C., Carlos, A., Azevedo, D., Bergmann, M., Meersmans, J., & Smith, P. (2019). Assessing the potential of soil carbonation and enhanced weathering through Life Cycle Assessment : A case study for Sao Paulo State , Brazil. Journal of Cleaner Production, 233, 468–481. https://doi.org/10.1016/j.jclepro.2019.06.099

Mant, R. C., Jones, D. L., Reynolds, B., Ormerod, S. J., & Pullin, A. S. (2013). A systematic review of the effectiveness of liming to mitigate impacts of river acidification on fish and macro-invertebrates. Environmental Pollution, 179, 285–293. https://doi.org/10.1016/j.envpol.2013.04.019

Many, G., Escoffier, N., Perolo, P., Bärenbold, F., Bouffard, D., & Perga, M. E. (2024). Calcite precipitation: The forgotten piece of lakes' carbon cycle. Science Advances, 10(44), eado5924. https://doi.org/10.1126/sciadv.ado5924

McQueen, N., Gomes, K. V., McCormick, C., Blumanthal, K., Pisciotta, M., & Wilcox, J. (2021). A review of direct air capture (DAC): Scaling up commercial technologies and innovating for the future. Progress in Energy, 3(3). https://doi.org/10.1088/2516-1083/abf1ce

Mercer, L., Burke, J., & Rodway-dyer, S. (2024). Towards improved cost estimates for monitoring, reporting and verification of carbon dioxide removal, London School of Economics and Political Science.

Meybeck, M., & Ragu, A. (1997). Presenting the GEMS-GLORI, a compendium of world river discharge to the oceans. Proceedings of Rabat Symposium S4. 243. 3-14. https://epic.awi.de/id/eprint/29205/

Moras, C. A., Bach, L. T., Cyronak, T., Joannes-Boyau, R., & Schulz, K. G. (2022). Ocean alkalinity enhancement - avoiding runaway CaCO3 precipitation during quick and hydrated lime dissolution. Biogeosciences, 19(15), 3537–3557. https://doi.org/10.5194/bg-19-3537-2022

Naturvårdsverket. (2011). Handbok för kalkning av sjöar och vattendrag. https://www.naturvardsverket.se/Documents/publikationer/978-91-620-0165-0.pdf

Palandri, J. L., & Kharaka, Y. K. (2004). A compilation of rate parameters of water-mineral interaction kinetics for application to geochemical modeling. USGS Open File Report, 2004–1068, 71. https://pubs.usgs.gov/of/2004/1068/#pdf

Parkhurst, D. L., & Appelo, C. A. J. (2013). Description of Input and Examples for PHREEQC Version 3 — A Computer Program for Speciation , Batch-Reaction , One-Dimensional Transport , and Inverse Geochemical Calculations (Techniques and Methods, Book 6, Chapter A43). U.S. Geological Survey.

Picot, B., Sambuco, J. P., Brouillet, J. L., & Riviere, Y. (2004). Wastewater stabilisation ponds: Sludge accumulation, technical and financial study on desludging and sludge disposal case studies in France. Water science & technology,51(12), 227–234. https://doi.org/10.2166/wst.2005.0469

Power, I. M., Hatten, V. N. J., Guo, M., Rausis, K., & Klyn-Hesselink, H. (2025). Are enhanced rock weathering rates overestimated? A few geochemical and mineralogical pitfalls. Frontiers in Climate, 6, 1510747. https://doi.org/10.3389/fclim.2024.1510747

Pypi.org. (2025). Searoute py. https://pypi.org/project/searoute/

Renforth, P. (2012). The potential of enhanced weathering in the UK. International Journal of Greenhouse Gas Control, 10, 229–243. https://doi.org/10.1016/j.ijggc.2012.06.011

Renforth, P. (2019). The negative emission potential of alkaline materials. Nature Communications, 10(1). https://doi.org/10.1038/s41467-019-09475-5

Renforth, P., Baltruschat, S., Peterson, K., Mihailova, B. D., & Hartmann, J. (2022). Using ikaite and other hydrated carbonate minerals to increase ocean alkalinity for carbon dioxide removal and environmental remediation. Joule, 6(12), 2674–2679. https://doi.org/10.1016/j.joule.2022.11.001

Renforth, P., & Henderson, G. (2017). Assessing ocean alkalinity for carbon sequestration. Reviews of Geophysics, 55(3), 636–674. https://doi.org/10.1002/2016RG000533

Rinder, T., & von Hagke, C. (2021). The influence of particle size on the potential of enhanced basalt weathering for carbon dioxide removal - Insights from a regional assessment. Journal of Cleaner Production, 315, 128178. https://doi.org/10.1016/j.jclepro.2021.128178

Rønning, J. (2024). Ocean Alkalinity Enhancement : A Tool to Mitigate Climate Change. https://doi.org/10.21996/p2f3-rp88

Sarno, L. Di, Majidian, A., & Karagiannakis, G. (2021). The Effect of Atmospheric Corrosion on Steel Structures. Buildings, 11(12), 571. https://doi.org/10.3390/buildings11120571

Scott, A., Oze, C., Shah, V., Yang, N., Shanks, B., Cheeseman, C., Marshall, A., & Watson, M. (2021). Transformation of abundant magnesium silicate minerals for enhanced CO2 sequestration. Communications Earth and Environment, 2(1). https://doi.org/10.1038/s43247-021-00099-6

Steinwidder, L., Boito, L., Frings, P. J., Niron, H., Rijnders, J., De Schutter, A., Vienne, A., and Vicca, S. (2025). Beyond Inorganic C: Soil Organic C as a Key Pathway for Carbon Sequestration in Enhanced Weathering. Global Change Biology, 31(7), e70340, https://doi.org/10.1111/gcb.70340

Sterling, S., Halfyard, E., Hart, K., Trueman, B., Grill, G., & Lehner, B. (2023). Addition of alkalinity to rivers: A new CO2 removal strategy [Preprint]. ESSOAr. https://doi.org/10.22541/essoar.168380809.92137625/v1

Sun, W., Jayaraman, S., Chen, W., Persson, K. A., & Ceder, G. (2015). Nucleation of metastable aragonite CaCO3 in seawater. Proceedings of the National Academy of Sciences of the United States of America, 112(11), 3199–3204. https://doi.org/10.1073/pnas.1423898112

The World Bank. (2025). state and trends of Carbon Pricing 2025. https://www.worldbank.org/en/publication/state-and-trends-of-carbon-pricing

Tian, M., Hartmann, J., Suitner, N., Amann, T., Kempe, S., Lim, C., & Moras, C. A. (2025). Stability of alkalinity in the land-ocean transition zone: A geochemical CDR perspective for the Elbe River, Germany. Environmental Research Letters. https://doi.org/10.1088/1748-9326/adeeab

Vienne, A., Frings, P., Poblador, S., Steinwidder, L., Rijnders, J., Schoelynck, J., Vinduskova, O., & Vicca, S. (2024). Earthworms in an enhanced weathering mesocosm experiment: Effects on soil carbon sequestration, base cation exchange and soil CO2 efflux. Soil Biology and Biochemistry, 199, 109596. https://doi.org/10.1016/j.soilbio.2024.109596

Vienne, A., Poblador, S., Portillo-estrada, M., Hartmann, J., Ijiehon, S., Wade, P., & Vicca, S. (2022). Enhanced Weathering Using Basalt Rock Powder : Carbon Sequestration , Co-benefits and Risks in a Mesocosm Study With Solanum tuberosum. Frontiers in Climate, 4, 869456, https://doi.org/10.3389/fclim.2022.869456

Wang, J., Keener, T. C., Li, G., & Khang, S. J. (1998). The dissolution rate of Ca(OH)2 in aqueous solutions. Chemical Engineering Communications, 169(1), 167–184. https://doi.org/10.1080/00986449808912726

Warbrick, C., Mcgoldrick, D., & Kirk, E. A. (1997). II. The 1996 protocol to the london dumping convention and the brent spar. International and Comparative Law Quarterly, 46(4), 957–964. https://doi.org/10.1017/S0020589300061303

Yan, Y., Dong, X., Li, R., Zhang, Y., Yan, S., Guan, X., Yang, Q., Chen, L., Fang, Y., & Zhang, W. (2023). Wollastonite addition stimulates soil organic carbon mineralization: Evidences from 12 land-use types in subtropical China. Catena, 225, 107031. https://doi.org/10.1016/j.catena.2023.107031

Zhang, S., Planavsky, N. J., Katchinoff, J., Raymond, P. A., Kanzaki, Y., Reershemius, T., & Reinhard, C. T. (2022). River chemistry constraints on the carbon capture potential of surficial enhanced rock weathering. Limnology and Oceanography, 67(S2), S148–S157. https://doi.org/10.1002/lno.12244

Supplementary material

Section 1: supplementary data

Table S1: Discharge weighed water use, cost per unit of net CDR and t rock required t-1 CDR.

η	type	compound	Water use (m^3/t CDR)	t rock / t CDR	$/t net CDR
0.65	**POND**	**$CaCO_3$**	43974.63	3.66	359.82
0.85	**POND**	**$CaCO_3$**	33770.65	2.80	241.02
0.65	**POND**	**$Ca(OH)_2$**	19742.91	1.49	627.05
0.85	**POND**	**$Ca(OH)_2$**	15810.44	1.15	301.73
0.65	**DIRECT**	**$CaCO_3$**	44161.62	3.66	208.10
0.85	**DIRECT**	**$CaCO_3$**	39822.92	2.87	149.12
0.65	**DIRECT**	**$Ca(OH)_2$**	20005.63	1.51	194.47
0.85	**DIRECT**	**$Ca(OH)_2$**	15785.00	1.15	123.28

Table S2: CDR potential for RAE in the 149 considered rivers after $CaOH_2$ addition up to a range of critical omegas (Ωc). Discharge weighed water consumption and maximum concentrations of $Ca(OH)_2$ to avoid $CaCO_3$ precipitation are also listed for different values of η (0.65 or 0.85).

Ωc	Gton gross CDR y^{-1}	m^3 t^{-1} CDR	η	$gCa(OH)_2$ L^{-1}
2.5	1.347	19743	0.65	0.089
2.5	1.761	15810	0.85	0.089
5.0	1.844	13151	0.65	0.121
5.0	2.411	10057	0.85	0.121
7.5	2.228	10826	0.65	0.146
7.5	2.913	8279	0.85	0.146
10.0	2.545	9525	0.65	0.167
10.0	3.328	7284	0.85	0.167

Table S3: Reaction schemes to illustrate CO_2 removal after (1) $CaCO_3$ dissolution (2) Ca_2SiO_4 dissolution (3) carbonate calcination and dissolution followed by carbonate precipitation.

$CaCO_3 + CO_2 + H_2O \Leftrightarrow 2HCO_3^- + Ca^{2+}$ 100% loss of initially captured CO_2 if $CaCO_3$ forms.	Reaction scheme 1
$Ca_2SiO_4 + 4\ CO_2 + 4H_2O \rightarrow 4\ HCO_3^- + 2Ca^{2+} + H_4SiO_4$ $4\ HCO_3^- + 2Ca^{2+} \Leftrightarrow 2\ CaCO_3 + 2\ H_2O + 2\ CO_2$ ---------- + $Ca_2SiO_4 + 2\ CO_2 + 2\ H_2O \rightarrow 2\ CaCO_3 + H_4SiO_4$ 50% loss of initially captured CO_2 if $CaCO_3$ forms.	Reaction scheme 2
$CaCO_3$ + heat $\rightarrow$ CO_2 (for CCS) + CaO $CaO + H_2O \rightarrow Ca(OH)_2$ (calcination) ---------- $Ca(OH)_2 \rightarrow 2\ OH^- + Ca^{2+}$ $2\ OH^- + 2\ H_2CO_3 \rightarrow 2\ HCO_3^- + 2\ H_2O$ $2HCO_3^- + Ca^{2+} \rightarrow CaCO_3 + H_2O + CO_2$ ---------- + $2\ H_2CO_3$ + heat $\Leftrightarrow$ CO_2 (CCS) + CO_2 (emitted) + $2\ H_2O$ Net effect if $CaCO_3$ forms and CCS is used: 50% loss of initially captured CO_2. Without CCS: 100% loss of initially captured CO_2.	Reaction scheme 3

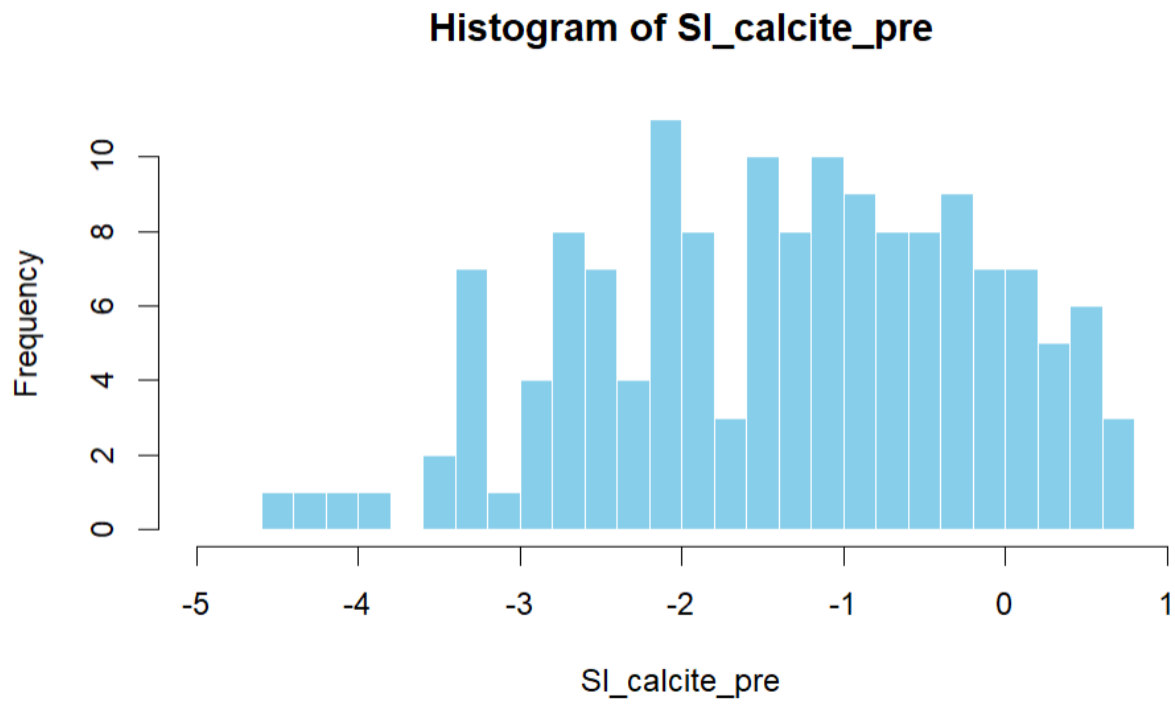

Figure S1: Histogram for saturation indexes of calcite before addition of limestone to the large rivers in this study.

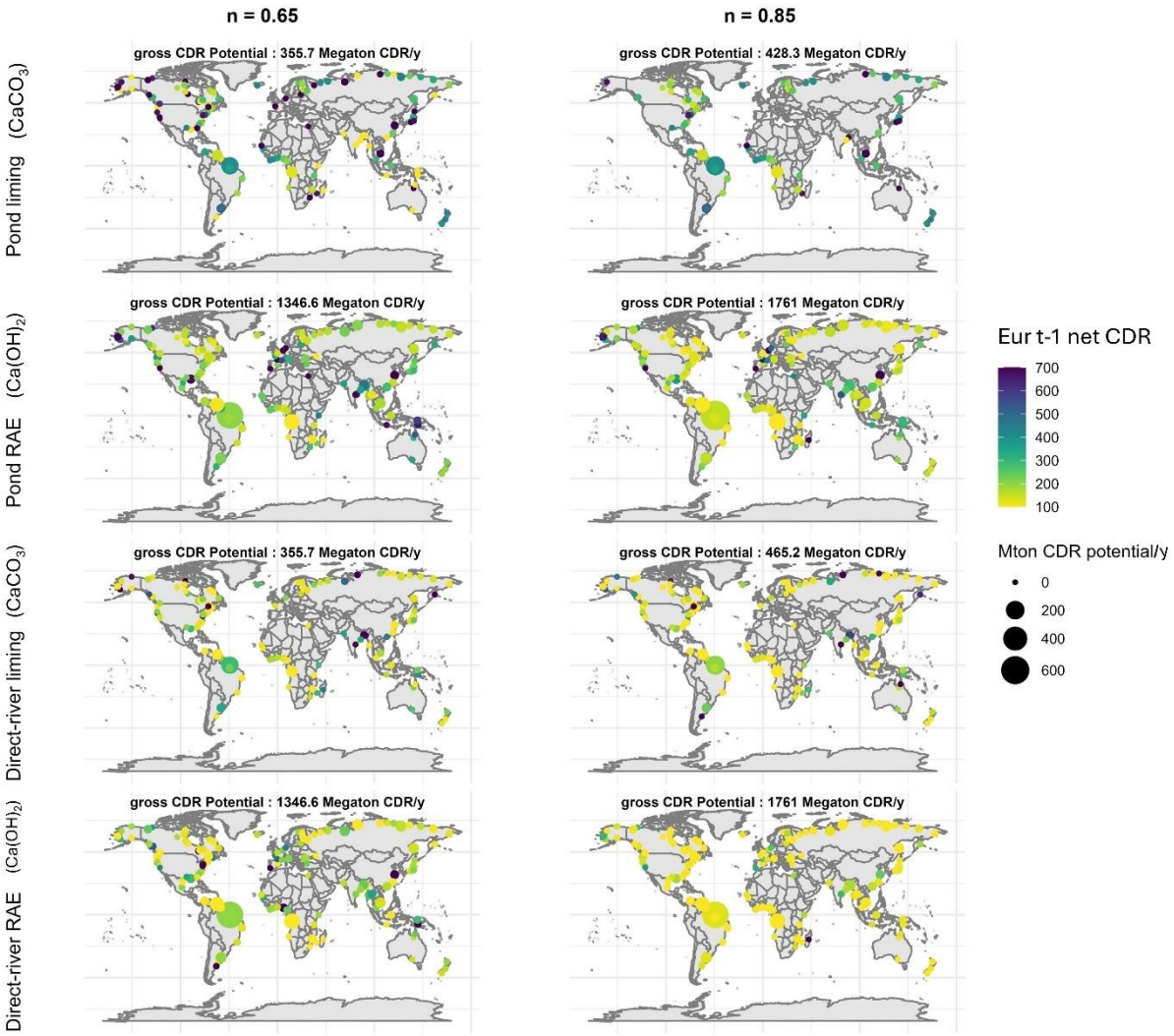

Figure S2: Gross CDR potential and the estimated cost for net CDR for large rivers accounting for 55% of the global freshwater discharge to the oceans for pond- and direct-river liming and direct-river $Ca(OH)_2$ addition. For RAE using $Ca(OH)_2$, a conservative Ωc threshold of 2.5 was assumed. In the left and right column, alkalinization efficiencies of 65 and 85% were assumed, respectively.

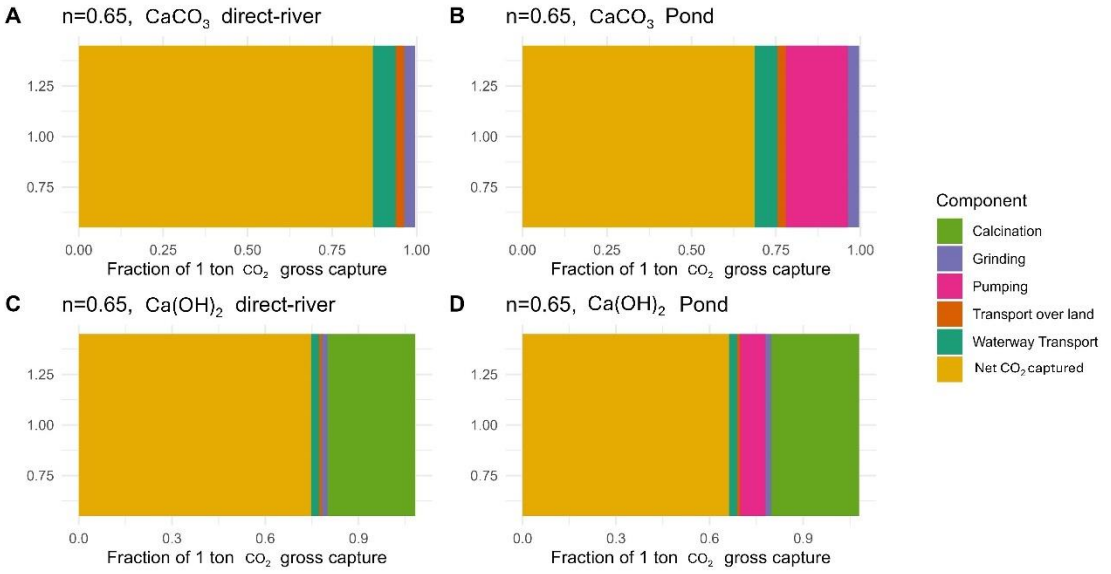

Figure S3: Life cycle emission overview for an alkalinization efficiency of 65% (the lowest efficiency of the considered range to visualize maximal relative life cycle emission penalties). Note that averages plotted here are regular averages of all investigated rivers and not discharge-weighted averages.

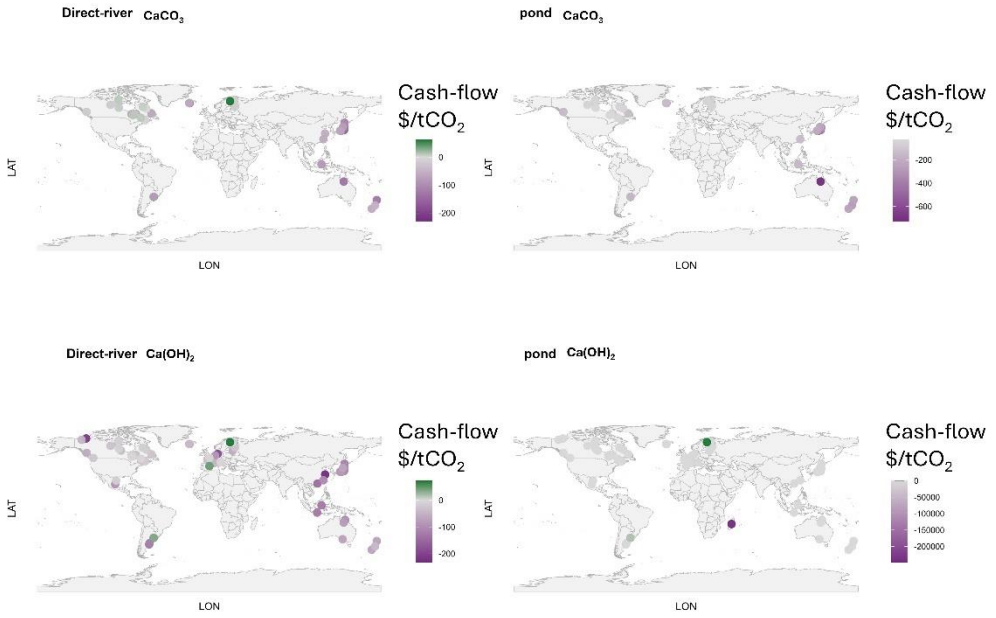

Figure S4: Cash flow (derived from the current CO_2 price minus the estimated cost of net CO_2 removal) for different locations globally. Green values indicate that profitable operation may be achieved assuming C-prices from 2025. The highest alkalization efficiency of our considered range (85%) was assumed here to assess at which locations, in the most optimistic case, RAE may generate positive cash flows. Rivers on locations where currently no C pricing / ETS scheme is in place are excluded from this Figure.

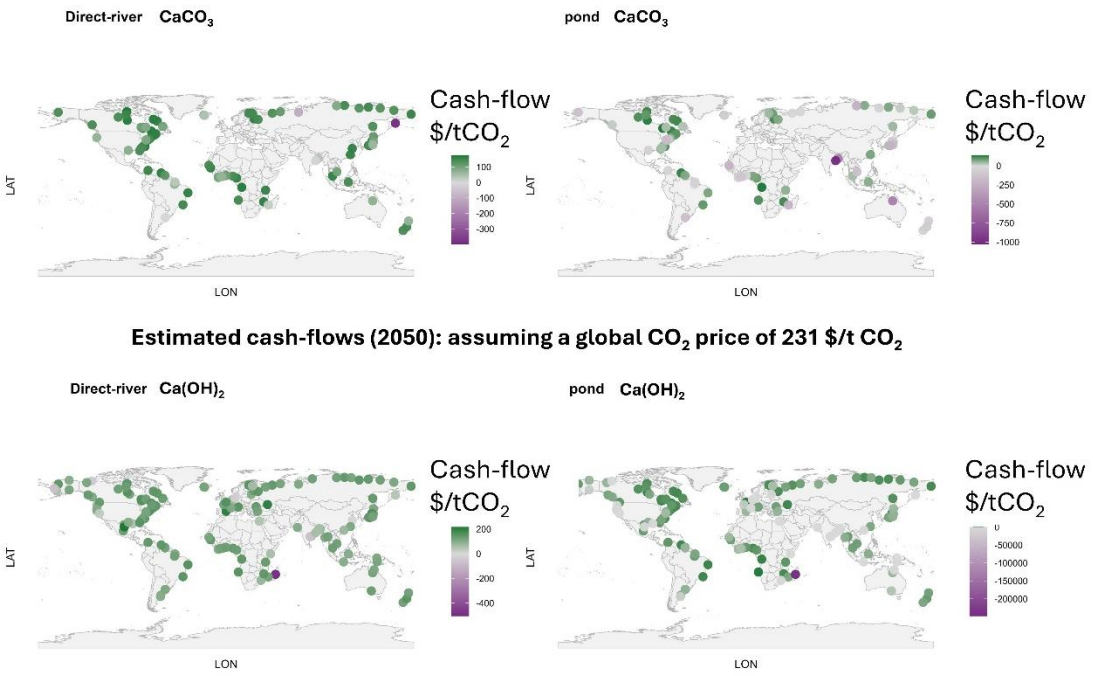

Figure S5: Cash-flows quantified with the global expected C price for 2050 of 231 $/ton CO_2. The highest alkalization efficiency of our considered range (85%) was assumed here to compare with Figure S4.

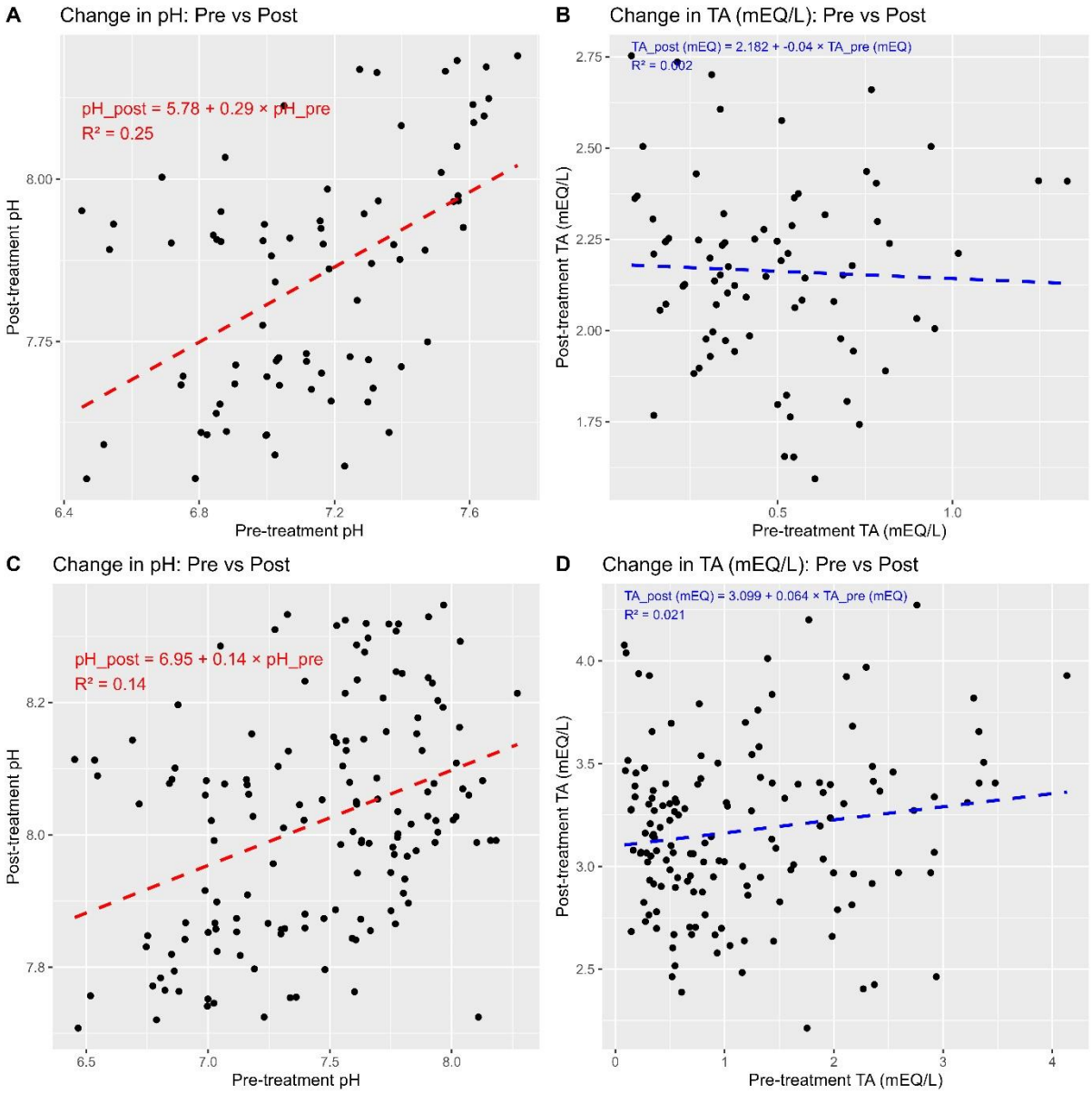

Figure S6: (A) pH and **(B)** total alkalinity (TA) of river mouth water compositions from the GEMS-GLORI database are shown on the x-axis, representing initial conditions. The corresponding values after addition of 2.27 ton of $CaCO_3$ (the theoretical amount required for 1 ton of CDR) to the volume needed for full dissolution are plotted on the y-axis. **(C)** and **(D)** show the same relationships, but after addition of $Ca(OH)_2$ to raise the calcite saturation state (Ω_calcite) up to 2.5.

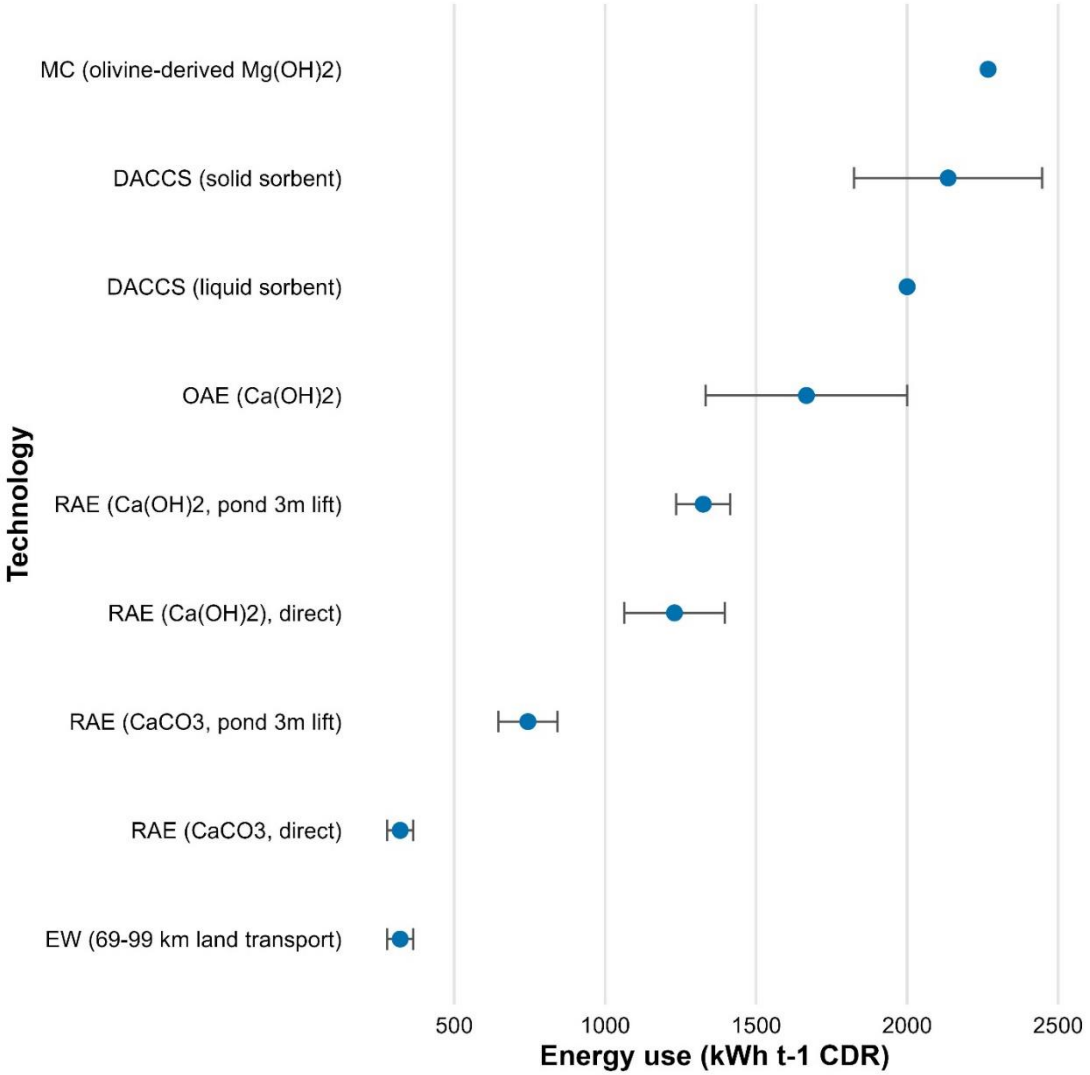

Figure S7: Overview of energy use of diverse geochemical CDR techniques with a comparison to DACCS. References for energy uses of different techniques can be found in the paragraphs below. For EW, we calculated the land transport distance so that the energy use per unit of CDR would be the same as with direct-river liming. References: for DACCS: (McQueen et al., 2021); MC with olivine-derived Mg(OH)2): (Scott et al., 2021); OAE= ocean liming in this figure (using $Ca(OH)_2$: Kowalczyk et al. (2024); RAE: discharge-weighed averages of this work, EW: (Rinder & von Hagke, 2021) and (Lefebvre et al., 2019). Dots without error bars represent best estimates, dots with error bars represent the mean of the range of reported energy uses. For the RAE scenarios, dots represent the average of the two outer alkalinization efficiency scenarios, which are represented by the upper and lower error bar. OAE= ocean alkalinity enhancement, RAE= river alkalinity enhancement. DACCS= direct-air carbon capture and storage, EW = Enhanced weathering, MC= mineral carbonation.

Section 2: Overview of coding files

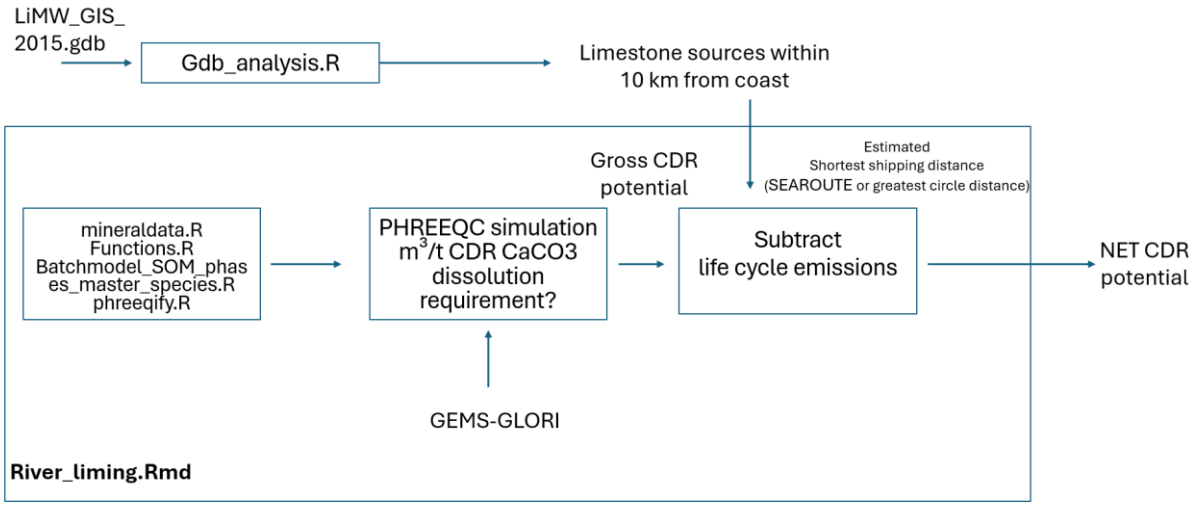

Figure S8: An overview of coding files and data sources used in this analysis. All code and required functions are available in zenodo.

Section 3: Process scheme

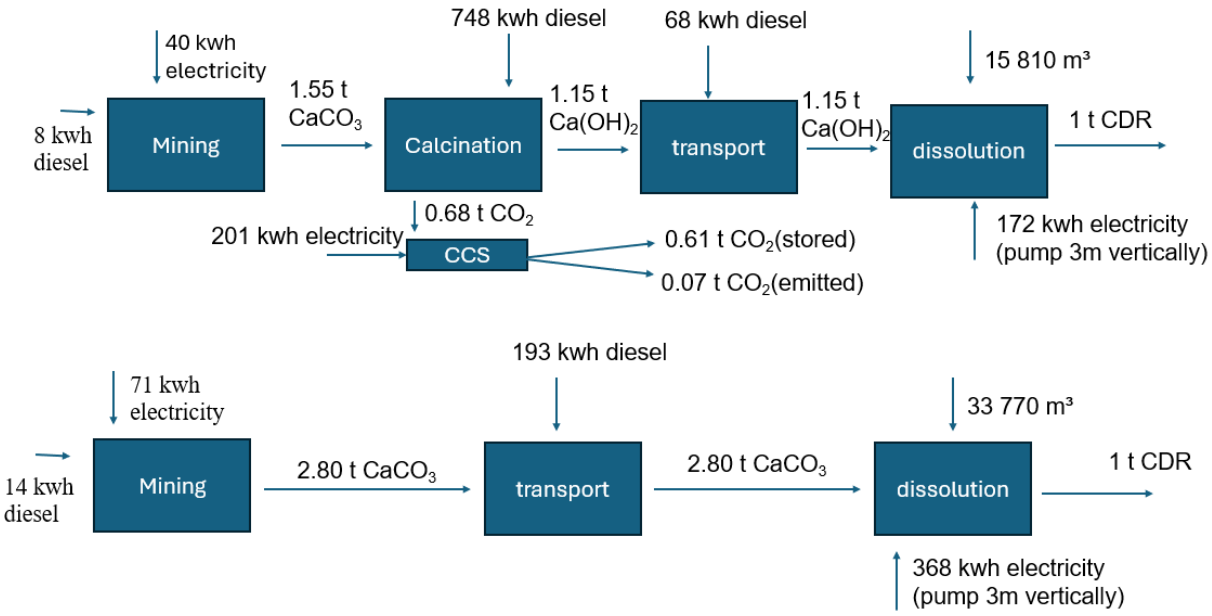

Figure S9: Process scheme/ overview of material and energetic inputs required to deliver 1 ton of gross CDR pond-river RAE for $Ca(OH)_2$ (top) and $CaCO_3$ (bottom). η=0.85 was assumed for this figure. For direct-river RAE values are similar yet exclude pumping electricity inputs. Energy values were taken from Table 1. Calcination was assumed to be complete. Water consumptions and the quantity of rock t^{-1} CDR are discharge-weighed averages (see **Table S1**).

Section 4: Sensitivity analyses

A sensitivity analysis was done to verify to what extent the results of our study depend on the assumptions that were made. First, we assumed that mixing was not required to maintain $CaCO_3$ in suspension during mineral dissolution. We assumed a 2.4 hours dissolution time for $CaCO_3$**.** Using stokes law (assuming laminar flow), we can estimate the settling velocity of 60 µm $CaCO_3$ particles (Equation S1):

$$v = \frac{2}{9} * \frac{r^2 * (rho_p - rho_f) * g}{\mu} \qquad Equation\ S1$$

With r= particle radius = 30 µm, rho_p = density $CaCO_3$ ~= 2700 kg/m³, rho_f= rho_fluid =~ 1000 kg / m³, g = 9.81 m/s², µ = viscosity (Pa.s).

We derive a settling velocity of 3.3 mm/s, which implies that $CaCO_3$ would settle in a 3 m depth pond within 15 minutes. If $Ca(OH)_2$ effectively dissolves 100 times faster than $CaCO_3$, then mixing may not be required for particles for $Ca(OH)_2$. Hence, despite the initial turbulence from pumping water in, and possibly some residual circulation, mixing would likely be required to keep $CaCO_3$ particles in suspension and prevent settling after this initial phase.

To keep fine solids in suspension 5 W per m³ is typically used for mixed liquor slurries in wastewater treatment. However, limited published data suggest that power levels much below the traditional design criteria (as low as 0.1 - 0.2 W/m³) are able to maintain adequate mixing (Pretorius et al., 2015). The lower the solids concentration and the finer the particle size, the lower the required revolutions per second of an impeller (N). The power of the mixer (in W/m³) then scales with N³, indicating that small increases in rotational speed led to disproportionately large increases in energy demand.

$$N = Sv^{0.1} * d^{0.2} * g * \left(\frac{rho_p - rho_f}{rho_f}\right)^{0.45} * X^{0.13} * D^{-0.85}$$

With Sv a constant for a given impeller and geometry that must be determined experimentally, d = particle diameter, g = 9.81 N/kg, rho_p and rho_f the densities of the particles and fluid respectively, D = impeller diameter and X = the concentration of suspended solids.

In wastewater treatment, mixed liquor suspended solids (MLSS) are typically 2-4 g/L (0.2-0.4 w%) and sludge particle size is typically in a similar range. For the $CaCO_3$ suspensions considered here, we assume an order of 1 ton $CaCO_3$ per 10 000 m³, giving concentrations in the order of 0.1 kg/m³ (or 0.01 w%). Based on the difference in X, we thus estimate that N is a factor two lower for CaCO3 than for MLSS. Nonetheless, also the particle density of the suspended organic flocs is likely less dense than minerals, so that the density factor $\left(\frac{rho_p - rho_f}{rho_f}\right)^{0.45}$ may roughly compensate the lower $X^{0.13}$ factor. In conclusion, these calculations suggest that power consumptions from mixed liquor system can be a good proxy for our envisioned $CaCO_3$ suspensions.

Given the likely comparability to mixed liquor systems and findings by Pretorius et al. (2015), we can estimate 0.5W/m³ or for a 10 000 m³ pond or thus 5 kW of power required per pond. When we assume continuous mixing over three hours, it would thus only require 15 kWh ton^{-1} $CaCO_3$ or about 42 kWh ton^{-1} CDR, and may thus add as much as 7% for pond- $CaCO_3$ (η=0.85). The added CAPEX for one mixer per pond with power in the range of several kW, is estimated to be in the order of 1000 $ mixer^{-1} (madeinchina, 2026) which is minor compared to the overall CAPEX of the ponds in our analysis.

Section 5: Spatial and Chemical Heterogeneity in Multi-Pond Deployment Assumptions

Secondly, the simulations assume a "single-extraction": all ponds withdraw river water from an identical extraction location and therefore experience the same background river chemistry. This assumption is unlikely to hold in practice, since only a limited fraction of a river's discharge can realistically be diverted at a single point. A more realistic implementation would likely consist of a sequence of ponds distributed over some geographic distance.

In such a configuration, downstream ponds would receive water that has already been chemically modified by upstream dissolution processes, leading to progressively higher alkalinity and cation concentrations compared to the original river background. In essence, the m^3/t CDR will increase gradually for pond-river RAE further downstream. Hence, also the pond pumping OPEX and CAPEX would increase further downstream, decreasing financial attractiveness gradually.

For direct-river RAE, no pumping OPEX or pond construction CAPEX are required; therefore, costs associated with direct-river RAE are not affected by the "single-extraction" assumption adopted in the main manuscript. The primary implication of this assumption would be a gradual reduction in the rate of rock dosage to rivers as baseline total alkalinity increases prior to rock addition. This would mainly influence the frequency of silo refilling and consequently the cumulative CDR achievable per silo, potentially affecting the discounted CAPEX expressed in $\$ t^{-1}$ CDR. Although reduced rock dosing would affect silo utilization, the overall cost implications remain limited. Silo infrastructure represented only a minor component of the total cost structure for direct-river RAE, which was dominated by energy and material transport expenses (Figure 4). Furthermore, our calculations assume refilling silos occurs once per week due to logistical constraints. In practice, these logistical limitations may be more restrictive than the gradual reduction in rock addition rates resulting from increasing upstream river alkalinity.

Section 6: Comparison of global riverine CDR estimates

Using $\Omega c = 5$, Zhang et al. 2022 report 2.5 Gt CO_2 yr^{-1} C transfer potential in rivers (through a terrestrial EW pathway), which is comparable to our 2.4 Gt CO_2 yr^{-1} gross CDR estimate for $Ca(OH)_2$ amendment, while we penalized with an alkalinity efficiency factor ($\eta = 0.85$). These numbers should be similar as the limiting factor is oversaturation of $CaCO_3$ in rivers in both analyses. Differences between our studies may reflect methodological choices; Zhang et al. (2022) used a GLORICH-based dataset from which certain rivers were filtered out, whereas our analysis is based on the GEMS-GLORI dataset, filtered to 149 major rivers representing ~55% of global runoff. Variations in discharge coverage and spatial representation of river chemistry likely contribute to the remaining discrepancies.

Section 7: Sensor sensitivity in ponds and for direct-river

This supplement details the step-by-step calculations used to assess the feasibility of detecting limestone ($CaCO_3$) dissolution using standard continuous Electrical Conductivity (EC) sensors (assumed accuracy of ±3%, after fulton et al. (2023)). We contrast the expected signal in a confined pond treatment system with a direct-river application, using the Amazon River as a boundary case. For a confined pond, we assume an operational target of 1 metric ton of CO_2 removal within a water body of approximately 30000 m^3. Removing 1 metric ton of CO_2 requires dissolving an equimolar amount of limestone.

- Moles of CO_2 = 1000000 g / 44.01 g/mol = 22722 moles
- Assuming equilibrium with CO_2 within a pond, this is equivalent to 22722 moles of Ca^{2+} and 45444 moles of HCO_3^- dissolution.

Dispersing these ions into a pond of 30 000 m^3 of water results in the following concentration increases (ΔC):

- $\Delta[Ca^{2+}]$ = 22,722 mol / 30000000 L = 0.757 mmol/L

- $\Delta[HCO_3^-]$ = 45444 mol / 30000000 L = 1.514 mmol/L

Using standard molar conductivities at 25°C (source: http://www.currentseparations.com/issues/18-3/cs18-3c.pdf), we quantify:

- Ca^{2+}contribution: 0.757 mM × 119.0 S.cm²/mol= 90.1 µS/cm
- HCO_3^- contribution: 1.514 mM × 44.5 S.cm²/mol = 67.4 µS/cm
- Total Expected Signal (ΔEC): ~157.5 µS/cm

Assuming a sensor scaled for a full-scale range of 1000 µS/cm a ±3% accuracy yields a maximum hardware error of ±30 µS/cm. The calculated dissolution signal (~157.5 µS/cm) is approximately 5 times larger than this error threshold, making $CaCO_3$ dissolution readily detectable in a controlled pond setup.

In a direct-river application, ions do however not accumulate in ponds; they are continuously flushed. Signal detection relies entirely on the ratio of the dosing rate to the river's volumetric flow rate. Let us consider the amazon as an extremely diluted river. To confidently exceed baseline noise and natural variance across an entire river profile using ±3% accuracy sensors, a differential spike of at least 30 µS/cm is required.

- 1 mmol/L of fully dissolved $CaCO_3$ yields 1 mmol Ca^{2+} and 2 mmol HCO_3^-, producing a combined EC boost of ~208 S.cm²/mol (119+2×44.5=208 S.cm²/mol).

- Target 30 µS/cm = 30 / 208 = 0.144230 mmol $CaCO_3$ should dissolve/L (=0. 144230 mol/m³)

Using the molar mass of $CaCO_3$ (100.09 g/mol), we calculate the mass of $CaCO_3$ needed to maintain this concentration increase in the entire Amazon flux. The Amazon River discharges approximately 200000 m³/second.

- Annual flux = 200000 m³/s × 31557600 s/year ≈ 6.31 × 10^{12} m³/year.

- For a 30 µS/cm signal:
  0.14423 mol/m³ × 100.09 g/mol × (6.31 × 10^12 m³/year) = 91 million metric tons/year

In conclusion, while a 30,000 m³ pond system easily yields a detectable ~157.5 µS/cm signal from just 1 ton of CO_2 equivalent dissolution, a direct-river application requires massive material inputs before an EC increase could be detected in rivers, highlighting the significant monitoring challenges of unconfined open-system alkalinity enhancement projects. Direct-river application in large rivers hence requires models. Dissolution tests (potentially in 'MRV ponds') using the exact river water chemistry at the envisioned location of direct-river application could aid in model parameterization.

Supplementary References

Fulton, S.G., Stegen, J.C., Kaufman, M.H., Dowd, J., & Thompson, A. (2023). Laboratory evaluation of open source and commercial electrical conductivity sensor precision and accuracy: How do they compare? PLOS ONE, 18(5), e0285092. https://doi.org/10.1371/journal.pone.0285092

Kowalczyk, K. A., Amann, T., Strefler, J., Vorrath, M. E., Hartmann, J., De Marco, S., Renforth, P., Foteinis, S., & Kriegler, E. (2024). SI: Marine carbon dioxide removal by alkalinization should no longer be overlooked. Environmental Research Letters, 19(7). https://doi.org/10.1088/1748-9326/ad5192

Lefebvre, D., Goglio, P., Williams, A., Manning, D. A. C., Carlos, A., Azevedo, D., Bergmann, M., Meersmans, J., & Smith, P. (2019). Assessing the potential of soil carbonation and enhanced weathering through Life Cycle Assessment : A case study for Sao Paulo State , Brazil. Journal of Cleaner Production, 233, 468–481. https://doi.org/10.1016/j.jclepro.2019.06.099

Made in China. (2026). *QJB type low speed liquid agitating/mixing submersible mixer for sewage treatment and water treatment system*. https://nl.made-in-china.com/co_submersible-mixer/product_Qjb-Type-Low-Speed-Liquid-Agitating-or-Mixing-Submersible-Mixer-for-Sewage-Treatment-and-Water-Treatment-System_yyuugrihng.html

McQueen, N., Gomes, K. V., McCormick, C., Blumanthal, K., Pisciotta, M., & Wilcox, J. (2021). A review of direct air capture (DAC): Scaling up commercial technologies and innovating for the future. Progress in Energy, 3(3). https://doi.org/10.1088/2516-1083/abf1ce

Pretorius, C., Wicklein, E., Rauch-Williams, T., Samstag, R., & Sigmon, C. (2015). How oversized mixers became an industry standard. *Proceedings of the Water Environment Federation*, *2015(11)*, 4379–4411. https://doi.org/10.2175/193864715819541747

Rinder, T., & von Hagke, C. (2021). The influence of particle size on the potential of enhanced basalt weathering for carbon dioxide removal - Insights from a regional assessment. Journal of Cleaner Production, 315, 128178. https://doi.org/10.1016/j.jclepro.2021.128178

Scott, A., Oze, C., Shah, V., Yang, N., Shanks, B., Cheeseman, C., Marshall, A., & Watson, M. (2021). Transformation of abundant magnesium silicate minerals for enhanced CO2 sequestration. *Communications Earth & Environment*, *2*, 25. https://doi.org/10.1038/s43247-021-00099-6